

3D geophysical joint inversion platform Tomofast-x

Vitaliy Ogarko, Jérémie Giraud, Roland Martin, Mark Jessell, Mark Lindsay
Kim Frankcombe, Taige Liu

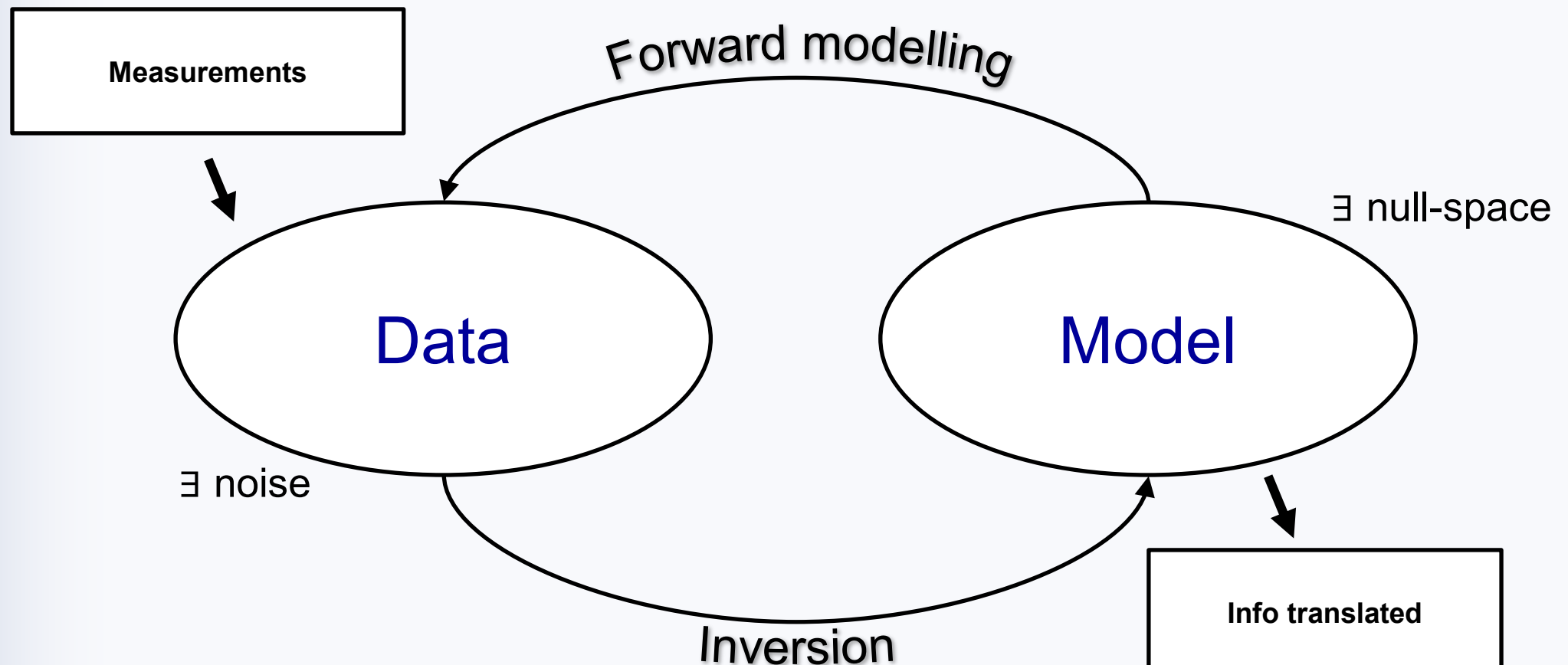
Centre for Exploration Targeting, School of Earth Sciences, The Uni. Of Western Australia, Crawley, Australia.

Géosciences Environnement Toulouse, GET, CNRS, Toulouse, France.

ExploreGeo - Geophysical Consultants to Explorers, Australia.

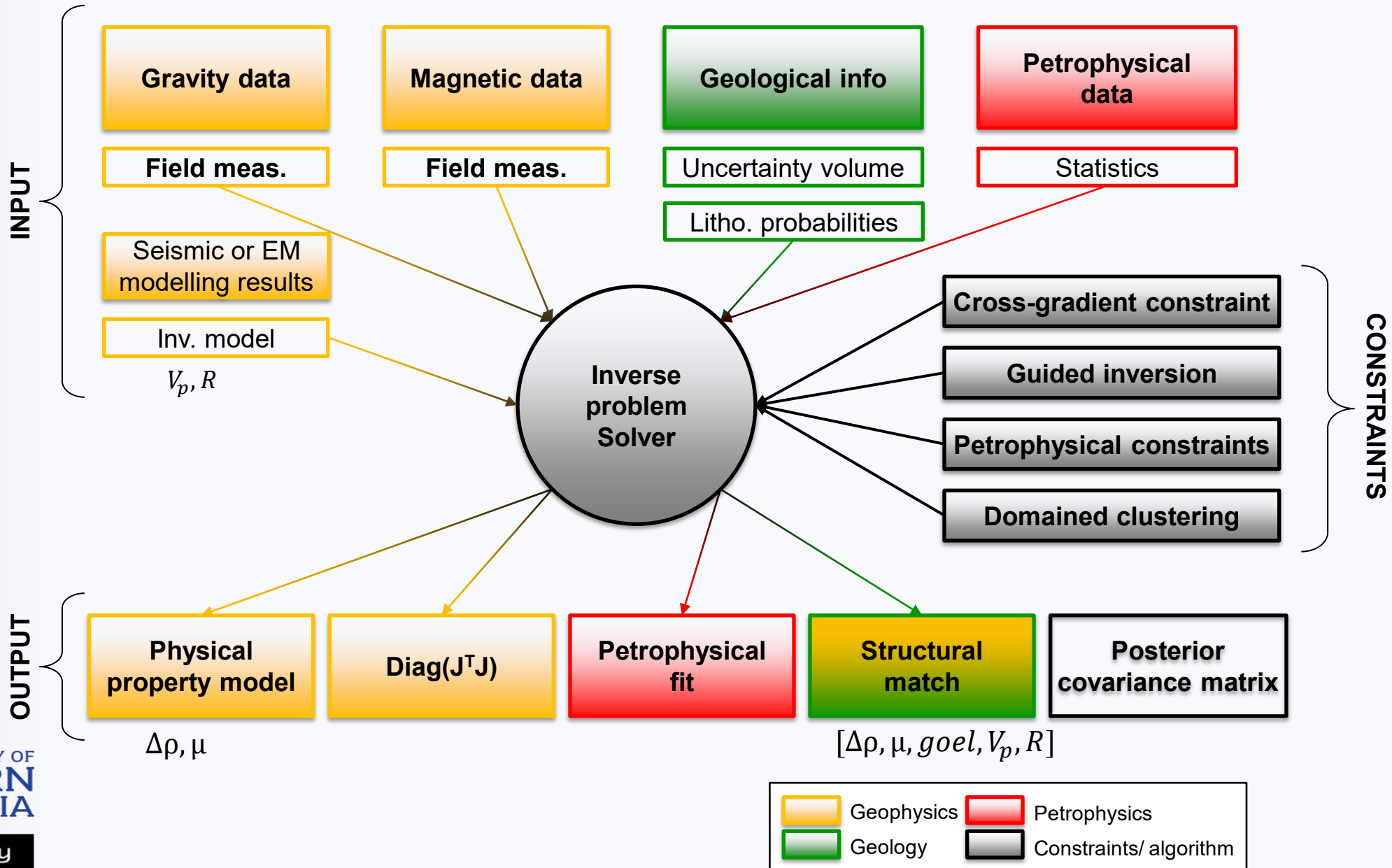
Contact: vitaliy.ogarko@uwa.edu.au

Inversion in a nutshell



Non-unique, can be tricky

Overview of Tomofast



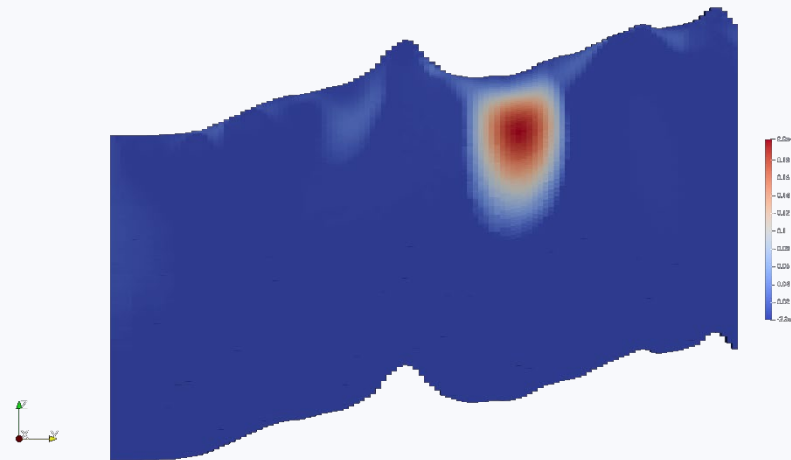
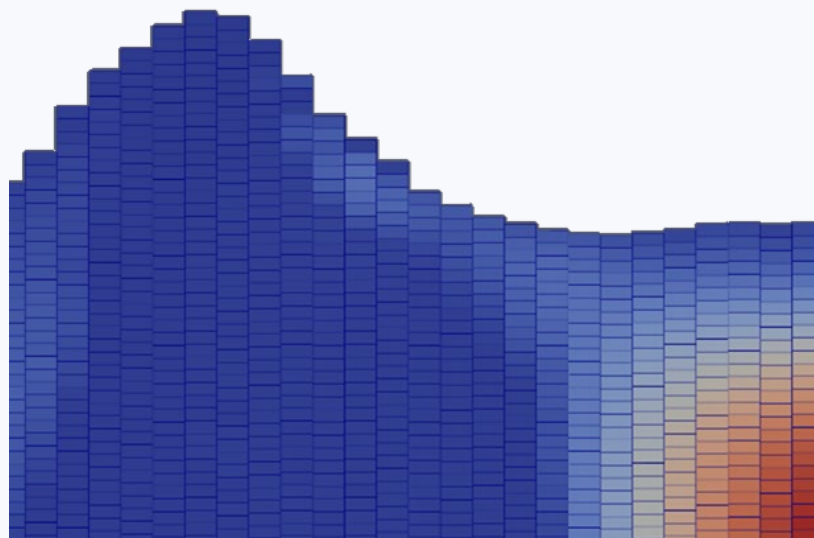
Code and Implementation (1/2)

- Fortran 2008
- Classes: objects, flexible
- 100% parallel (MPI)
- Vectorized → fast
- Unit tests
- Github
 - user manual
 - publications
 - datasets
- Cross-platform
 - Makefile: Linux, WSL, MacOS
- Cross-compile
 - GCC, Intel
- No dependencies but MPI



Code and Implementation (2/2)

- Topography
 - terrain following mesh
- Memory reduction
 - Wavelet compression
- I/O
 - Paraview (vtk)
 - Python/Matlab
- Parameter file
 - Flexible – input only the necessary



Formulation

$$\theta(\mathbf{d}, \mathbf{m})$$

$$= \alpha_d \left\| \mathbf{W}_d (\mathbf{d} - \mathbf{g}(\mathbf{m})) \right\|_{L_2}^2 \leftarrow \text{Data}$$

$$+ \alpha_m \left\| \mathbf{W}_m (\mathbf{m} - \mathbf{m}_{pr}) \right\|_{L_p}^2 \leftarrow \text{Prior model}$$

$$+ \alpha_g \left\| \mathbf{W}_g \nabla \mathbf{m} \right\|_{L_2}^2 \leftarrow \text{Smoothness}$$

$$+ \alpha_x \left\| \mathbf{W}_x (\nabla \mathbf{m}_1 \times \nabla \mathbf{m}_2) \right\|_{L_2}^2 \leftarrow \text{Cross-gradient}$$

$$+ \alpha_{pe} \left\| \mathbf{W}_{pe} \mathbf{P}(\mathbf{m}) \right\|_{L_2}^2 \leftarrow \text{Petrophysics}$$

$$+ \alpha_a \left\| \mathbf{W}_a (\mathbf{m} - \mathbf{v} + \mathbf{u}) \right\|_{L_2}^2 \leftarrow \text{ADMM/clustering}$$

Each term = Parameter file section

Formulation

$$\begin{aligned}\theta(d, m) \\ = \alpha_d \|W_d(d - g(m))\|_{L_2}^2 &\leftarrow \text{Data} \\ + \alpha_m \|W_m(m - m_{pr})\|_{L_p}^2 &\leftarrow \text{Prior model}\end{aligned}$$

```
=====
DATA parameters
=====
forward.data.grav.nData      = 256
forward.data.grav.dataGridFile = data/gravmag/mansf_slice/data_grid.txt
forward.data.grav.dataValuesFile = output/mansf_slice/grav_calc_read_data.txt

=====
MODEL DAMPING (m - m_prior)
=====
inversion.modelDamping.grav.weight = 1.d-11
inversion.modelDamping.normPower = 2.0d0
```

Each term = Parameter file section

Tomofast-x v1.0 release paper

Geosci. Model Dev., 14, 6681–6709, 2021
<https://doi.org/10.5194/gmd-14-6681-2021>
© Author(s) 2021. This work is distributed under
the Creative Commons Attribution 4.0 License.

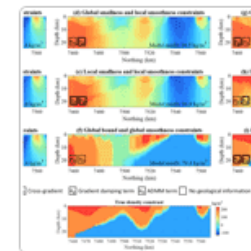
Article Assets Peer review Metrics Related articles



Development and technical paper

02 Nov 2021

Structural, petrophysical, and geological constraints in potential field inversion using the Tomofast-x v1.0 open-source code



Jérémie Giraud^{1,2,a}, Vitaliy Ogarko^{1,2,3}, Roland Martin⁴, Mark Jessell^{1,2}, and Mark Lindsay^{1,2}

¹Centre for Exploration Targeting (School of Earth Sciences), University of Western Australia, 35 Stirling Highway, 6009 Crawley, WA, Australia

²Mineral Exploration Cooperative Research Centre, School of Earth Sciences, University of Western Australia, 35 Stirling Highway, 6009 Crawley, WA, Australia

³The International Centre for Radio Astronomy Research, University of Western Australia, 7 Fairway, 6009 Crawley, WA, Australia

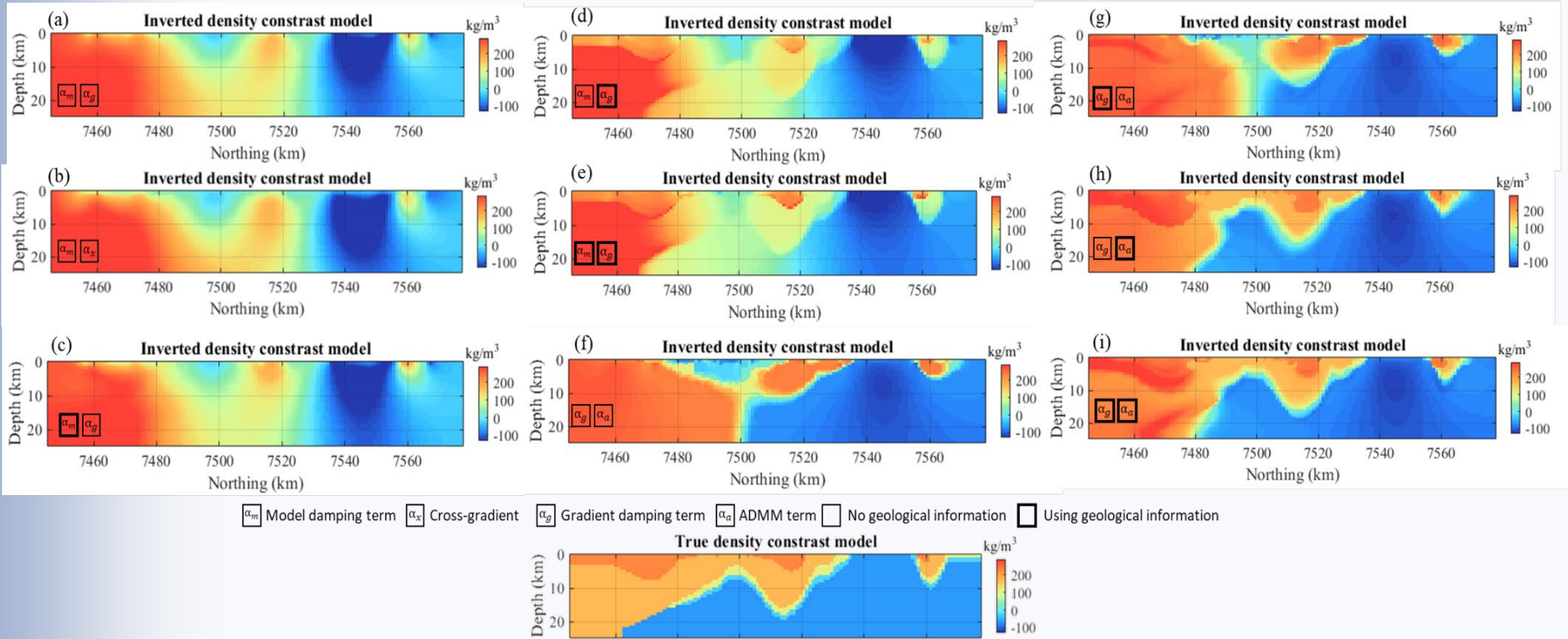
⁴Laboratoire de Géosciences Environnement Toulouse GET, CNRS UMR 5563, Observatoire Midi-Pyrénées, Université Paul Sabatier, 14 avenue Edouard Belin, 31400, Toulouse, France

^anow at: GeoRessources, Université de Lorraine, CNRS, 54000, Nancy, France

Correspondence: Jérémie Giraud (jeremie.giraud@uwa.edu.au)

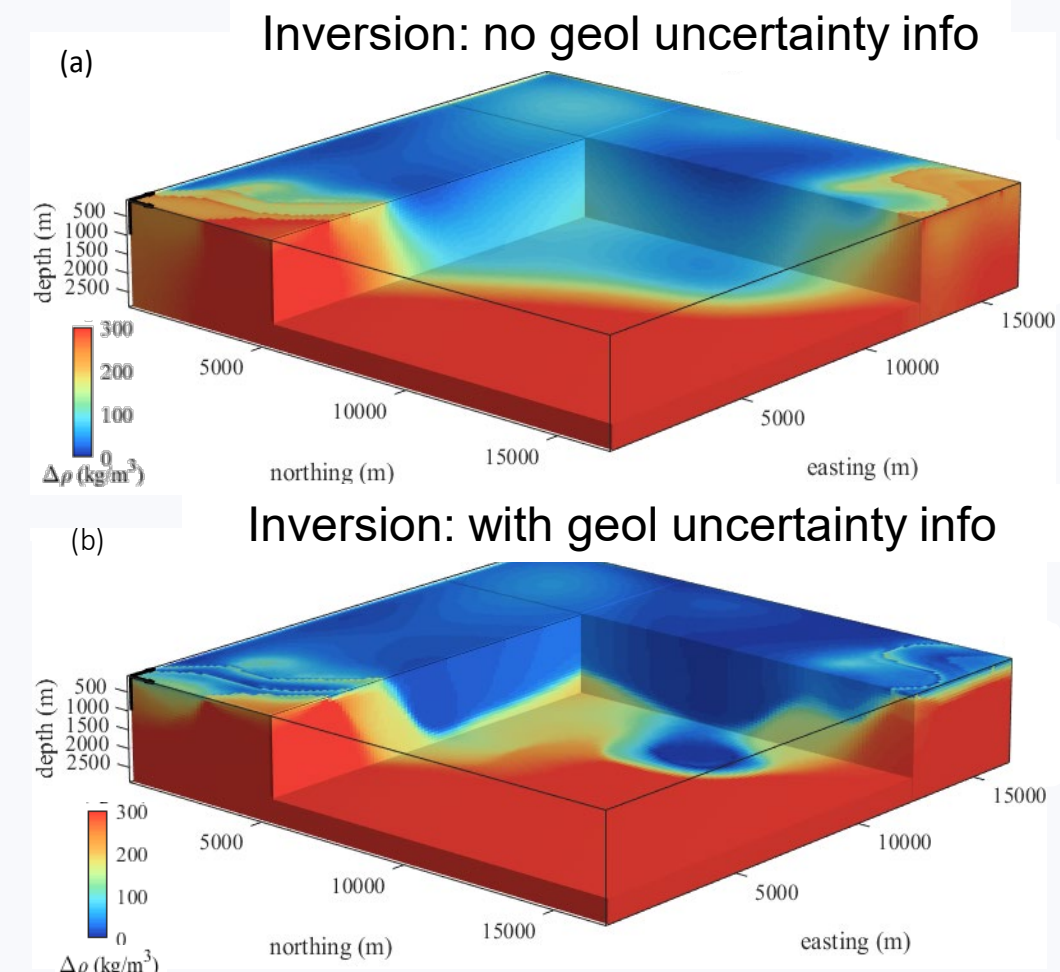
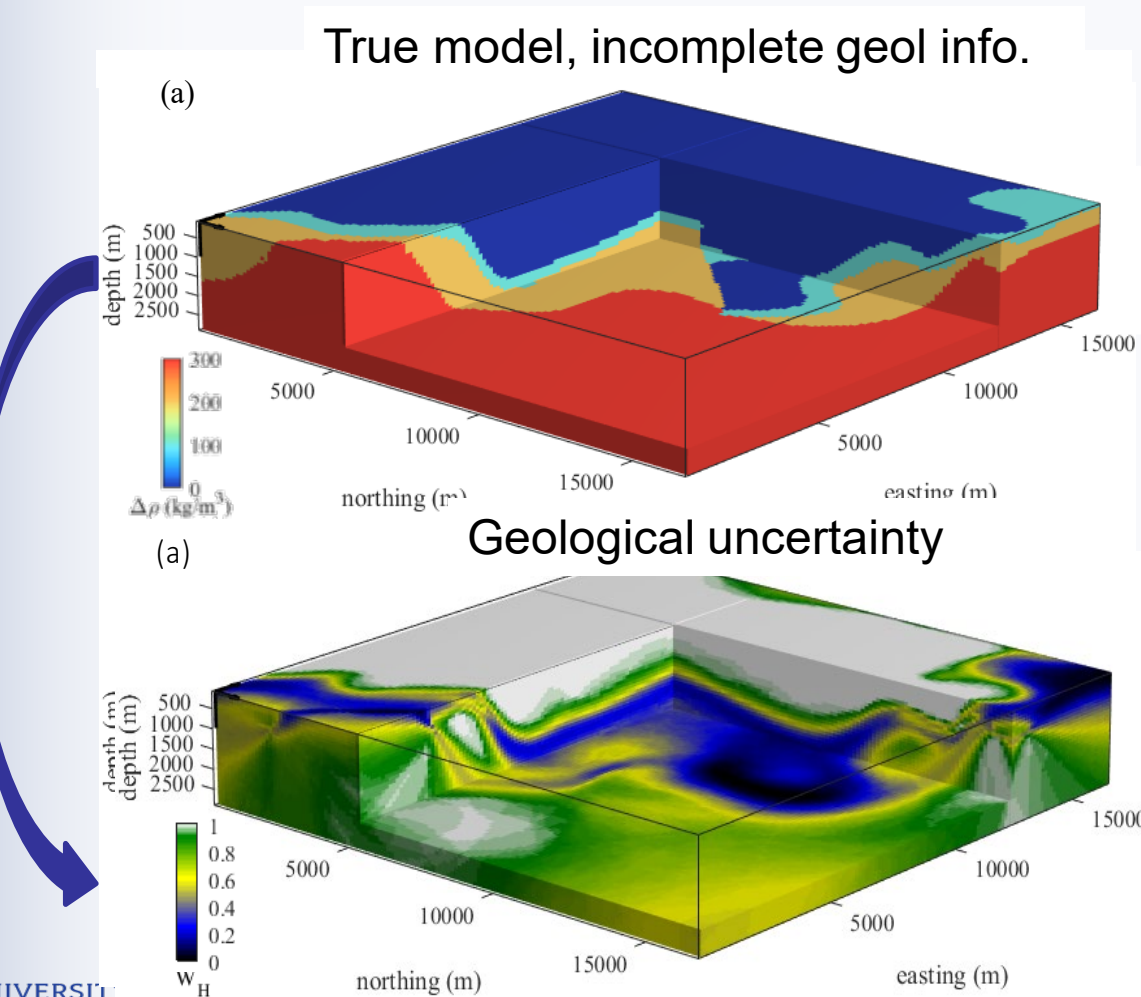
Received: 21 Jan 2021 – Discussion started: 30 Mar 2021 – Revised: 22 Jul 2021 – Accepted: 23 Jul 2021 – Published: 02 Nov 2021

Different types of constraints

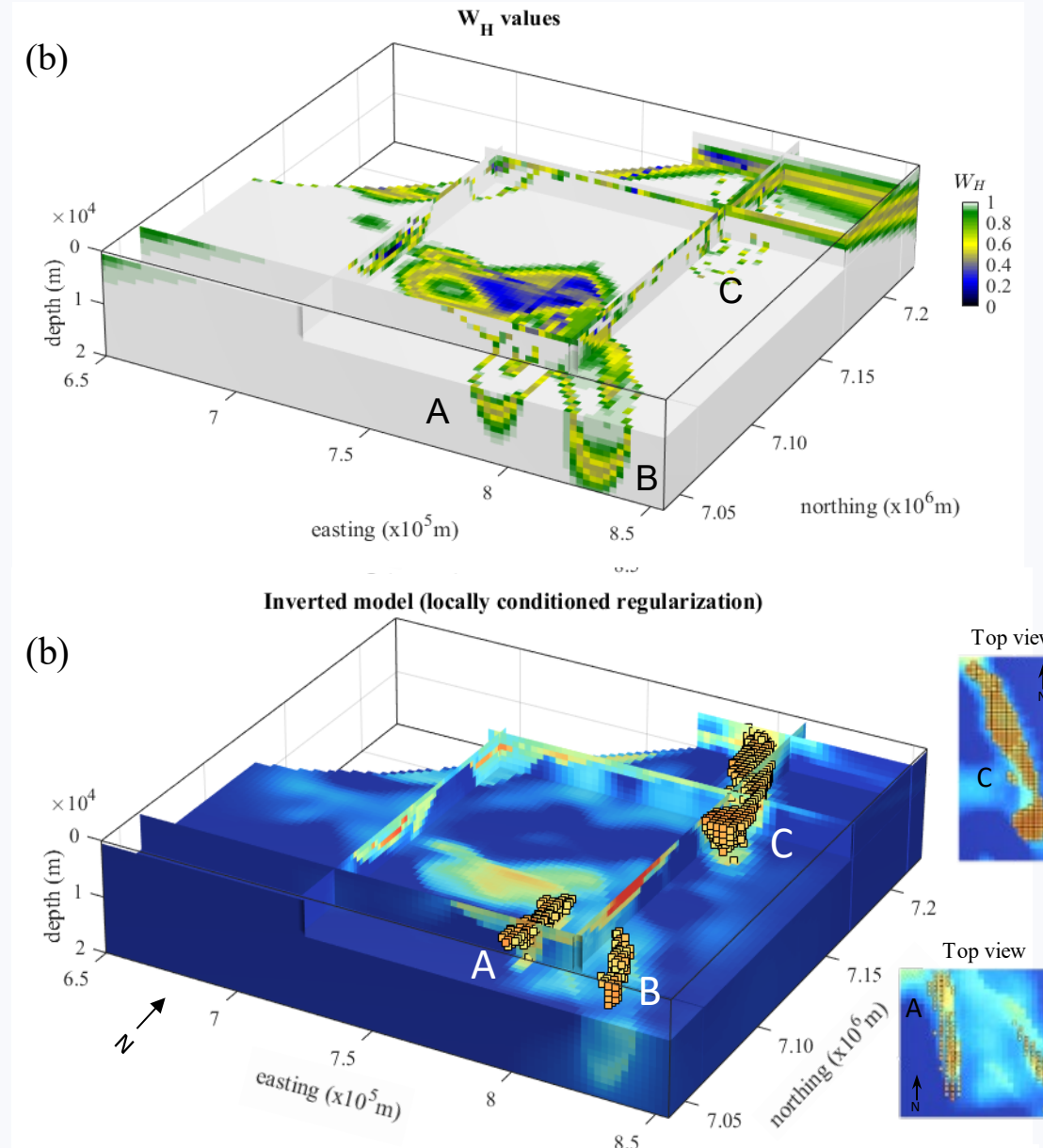
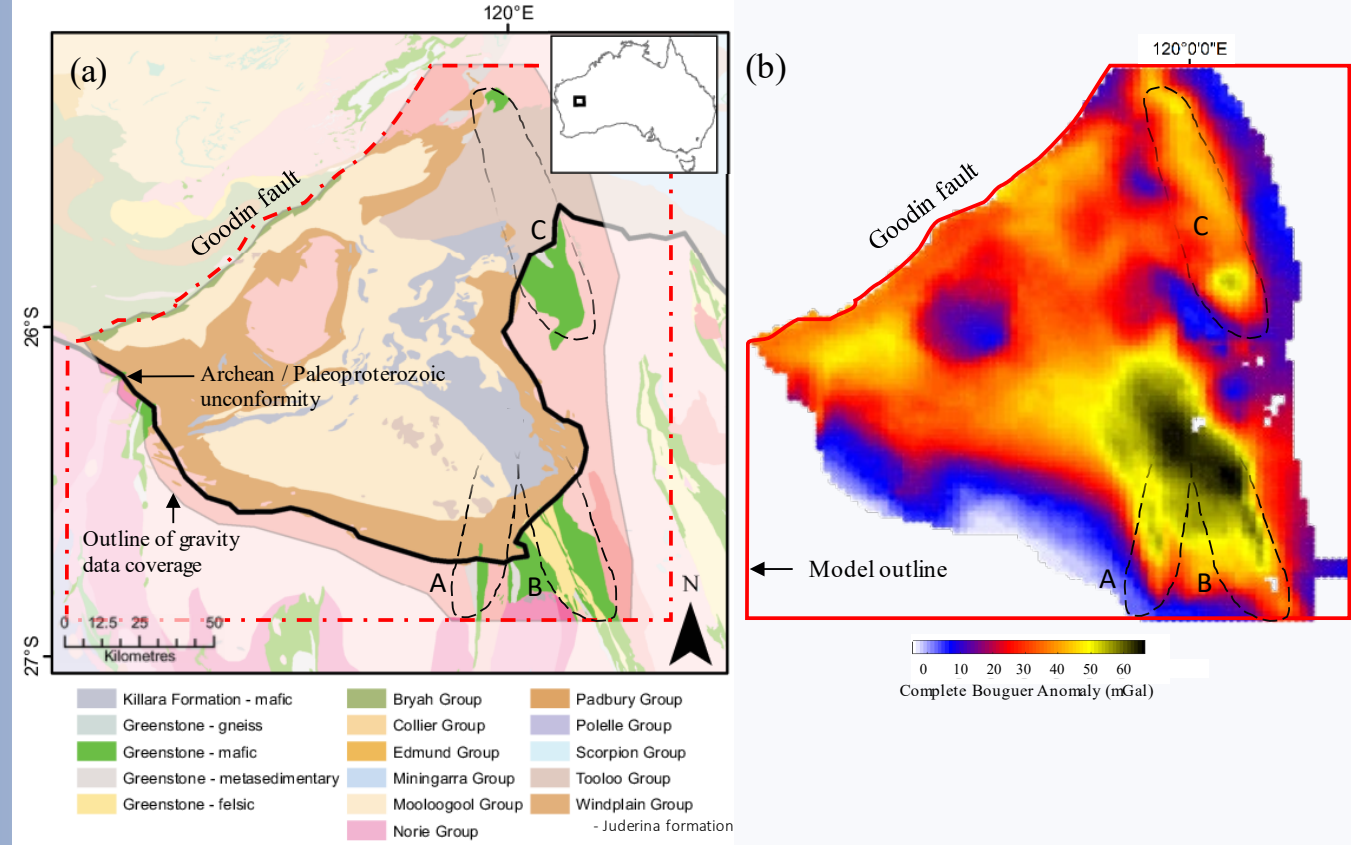


Local gradient regularization

McMC on
geology



Local gradient regularization



Cross gradient constraints

JOURNAL ARTICLE

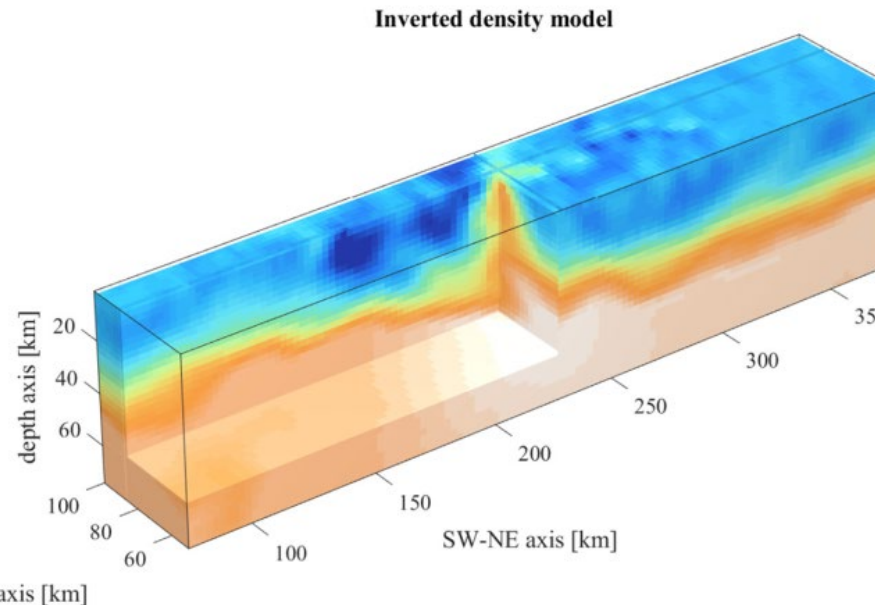
Three-dimensional gravity anomaly data inversion in the Pyrenees using compressional seismic velocity model as structural similarity constraints

 Get access >

Roland Martin , Jérémie Giraud, Vitaliy Ogarko, Sébastien Chevrot, Stephen Beller, Pascal Gégout, Mark Jessell

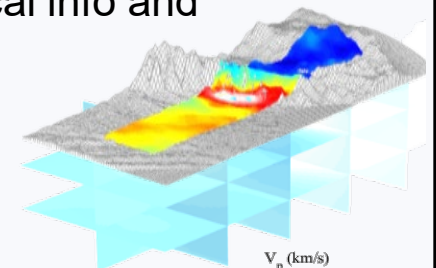
Geophysical Journal International, Volume 225, Issue 2, May 2021, Pages 1063–1085,
<https://doi.org/10.1093/gji/ggaa414>

Published: 01 September 2020 Article history ▾

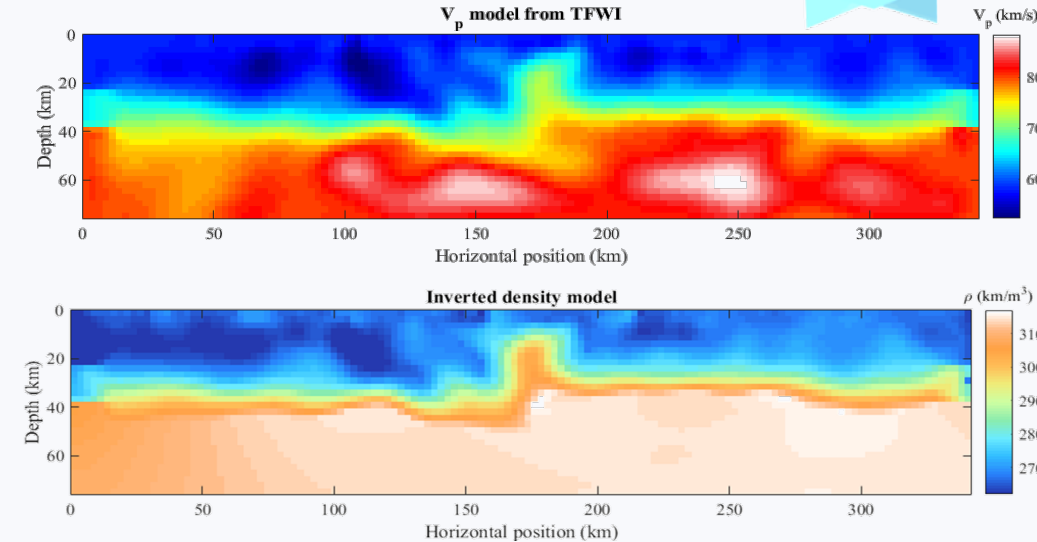


Cross-gradient with V_p

- Exploit structural and petrophysical info and horizontal resolution of seismic
- Reconcile different geophysics



Western Pyrenees, France/Spain



Martin et al. 2020 *in review.*

Petrophysical constraints

JOURNAL ARTICLE

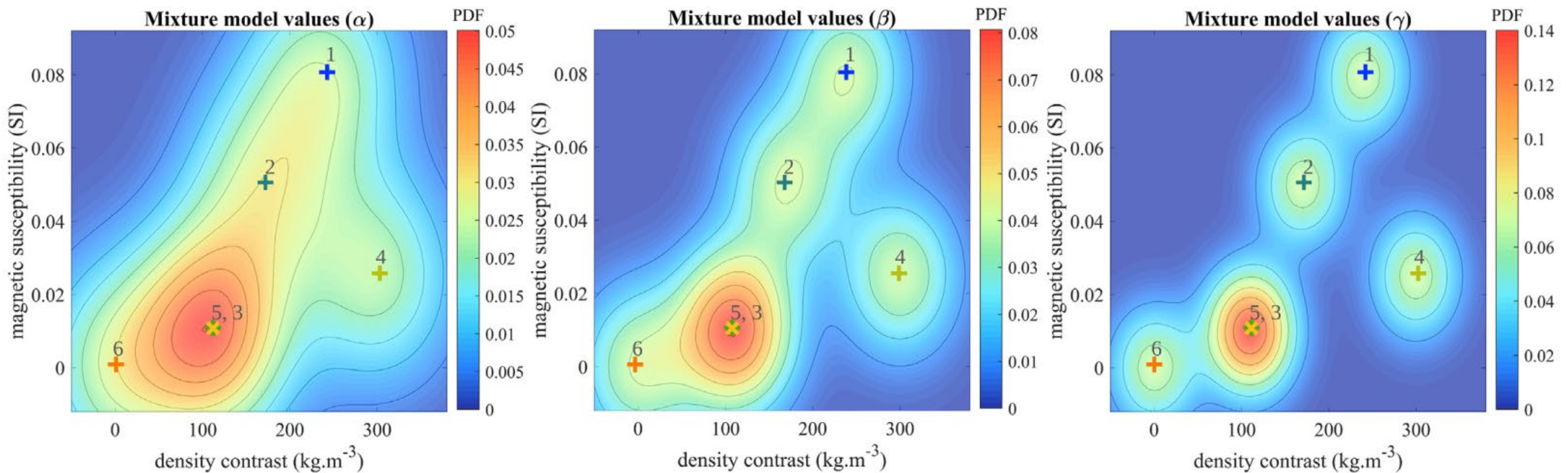
Sensitivity of constrained joint inversions to geological and petrophysical input data uncertainties with posterior geological analysis

Jérémie Giraud , Vitaliy Ogarko, Mark Lindsay, Evren Pakyuz-Charrier, Mark Jessell, Roland Martin

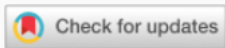
Geophysical Journal International, Volume 218, Issue 1, July 2019, Pages 666–688,

<https://doi.org/10.1093/gji/ggz152>

Published: 27 March 2019 Article history ▾



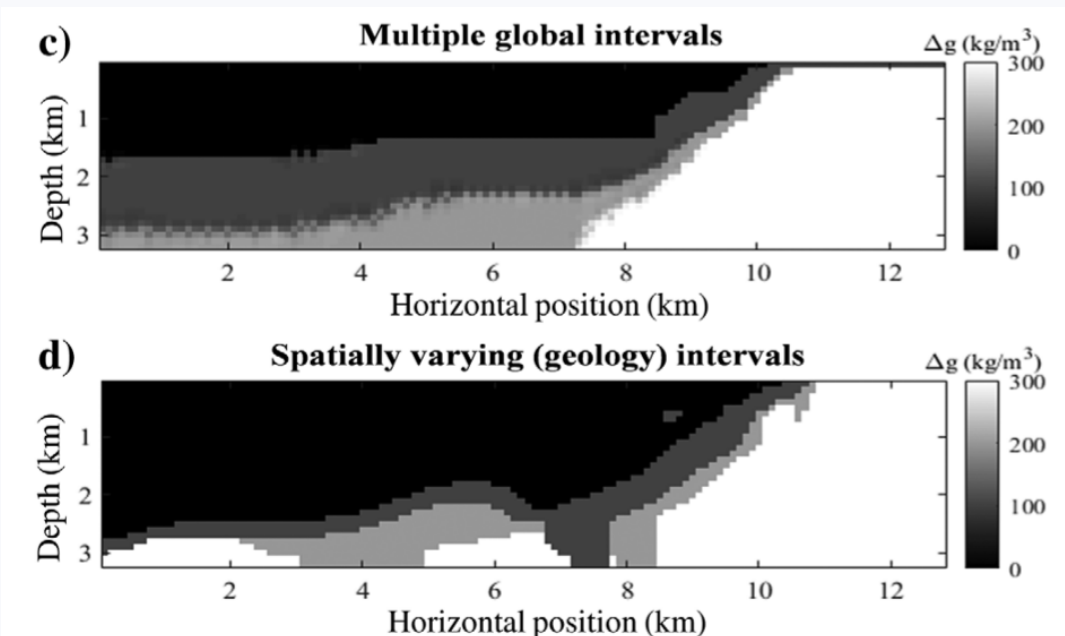
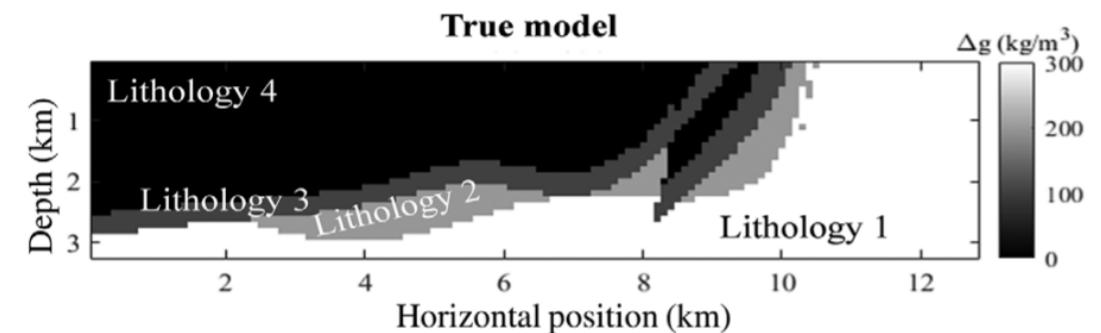
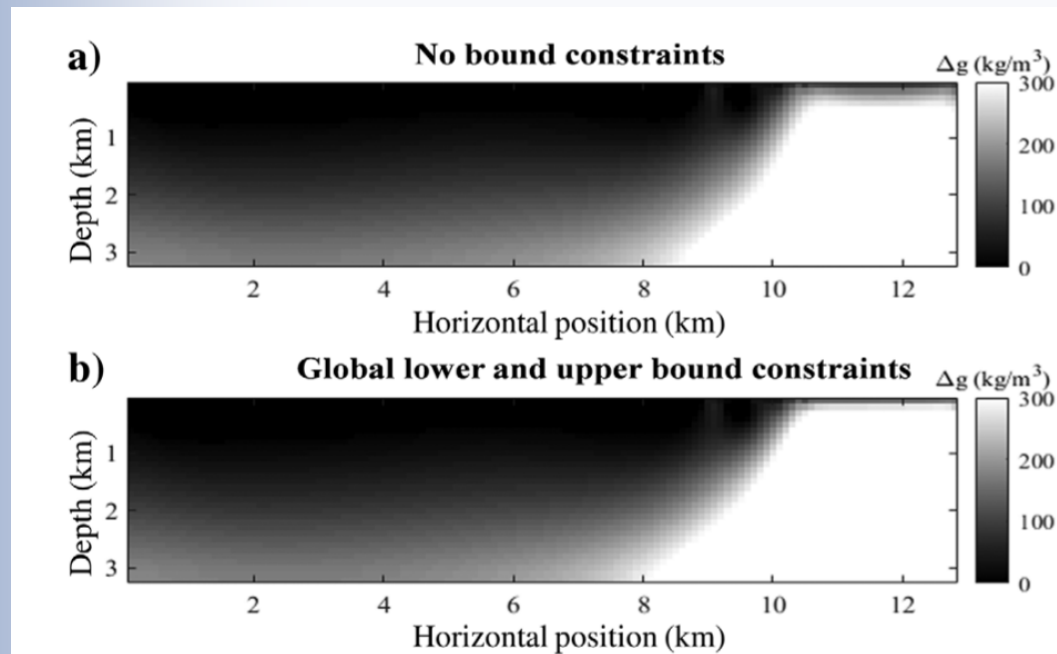
Disjoint interval bound constraints using the alternating direction method of multipliers for geologically constrained inversion: Application to gravity data

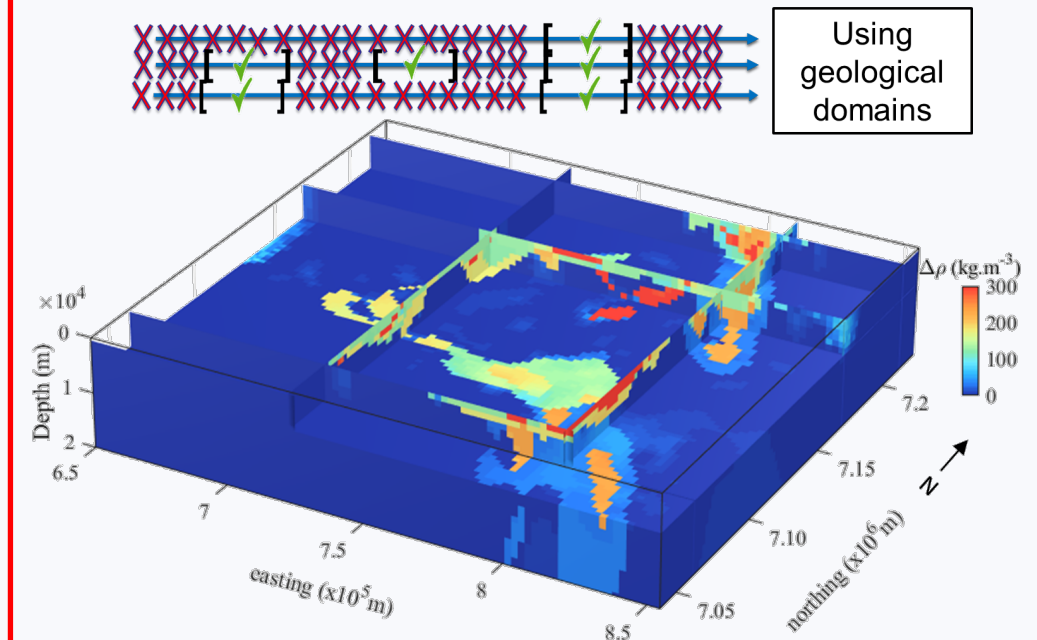
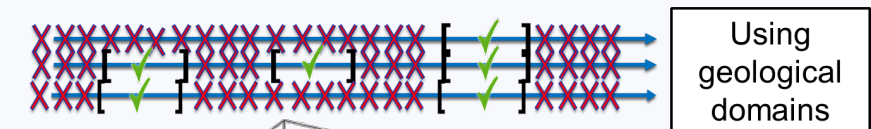
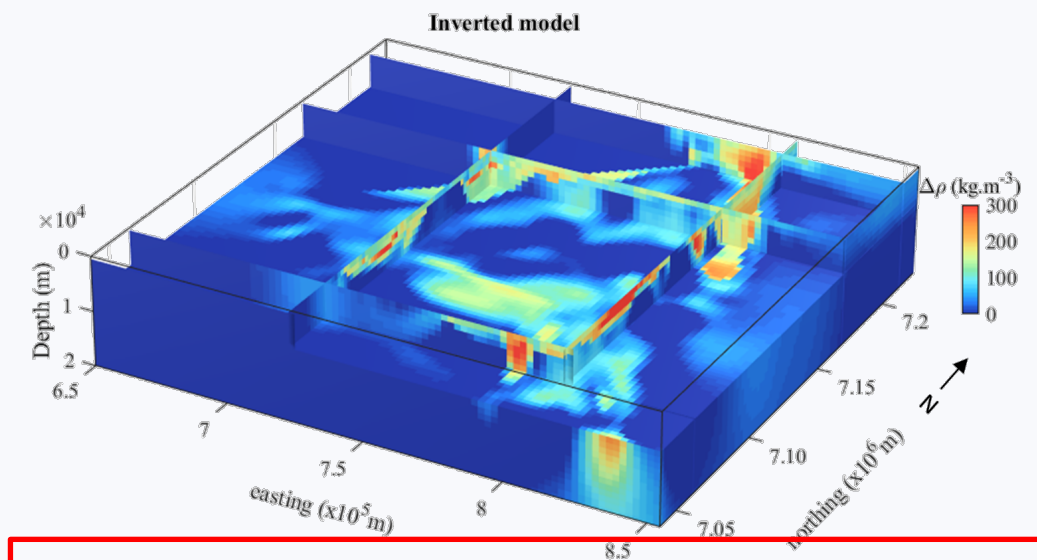
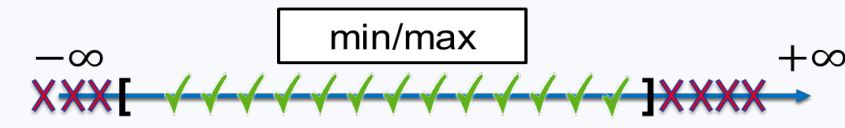
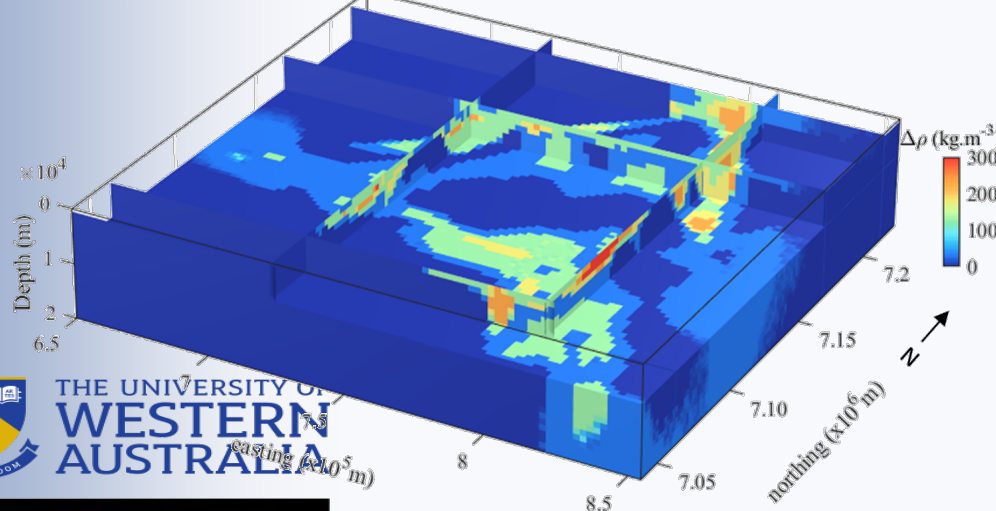
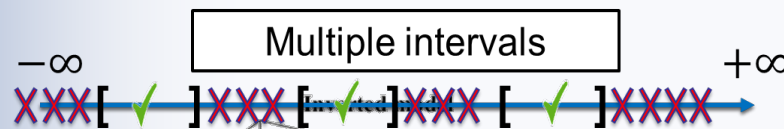
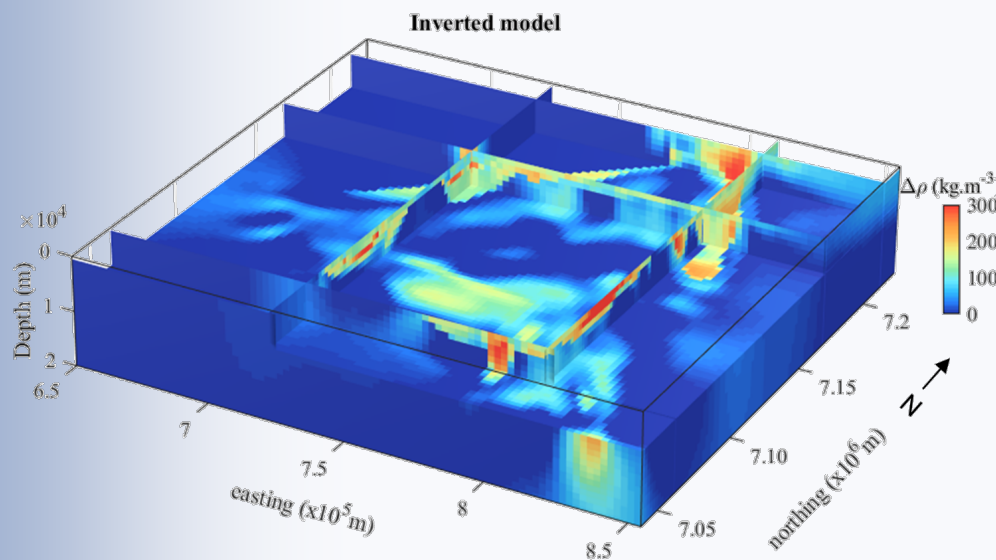


Authors:

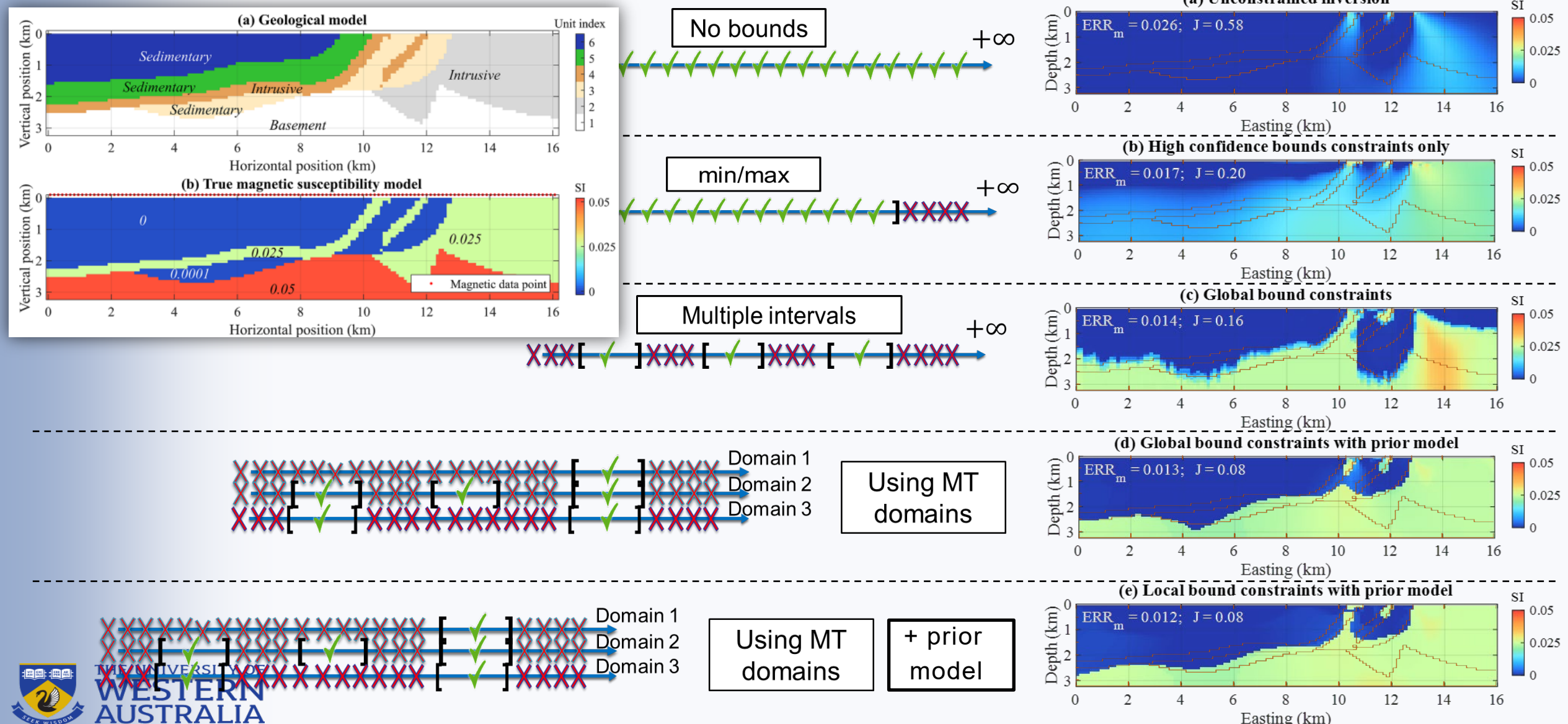
Vitaliy Ogarko , Jérémie Giraud , Roland Martin , and Mark Jessell

<https://doi.org/10.1190/geo2019-0633.1>





Using MT to constrain magnetic inversion

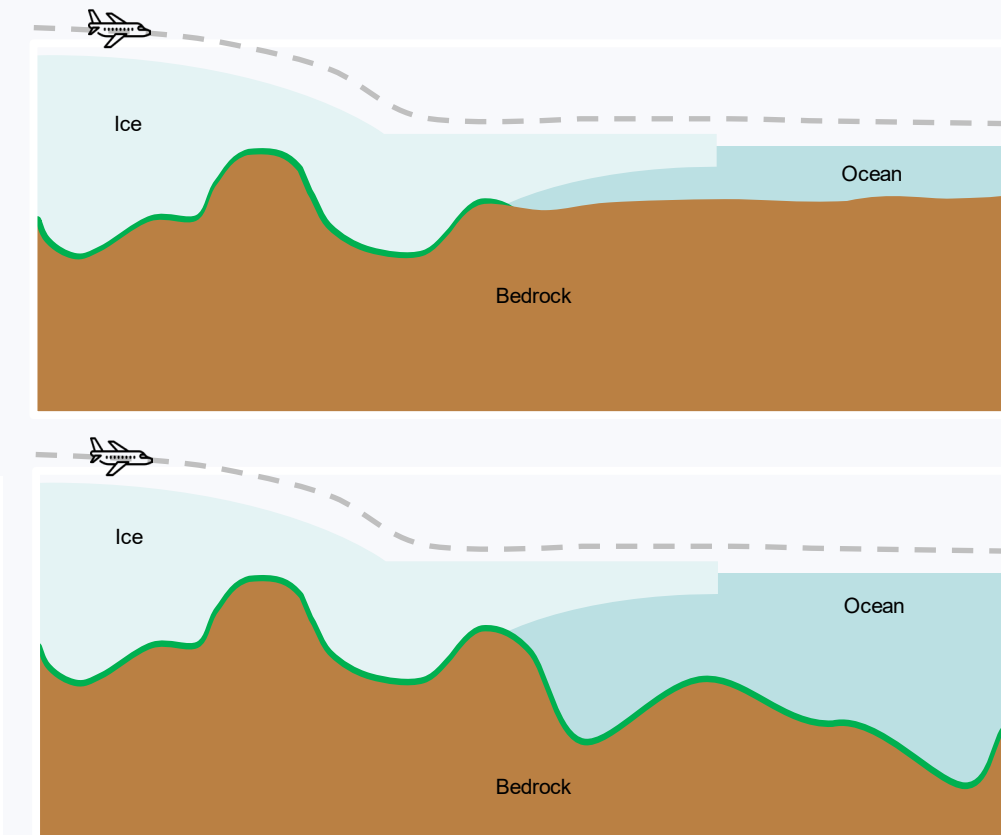
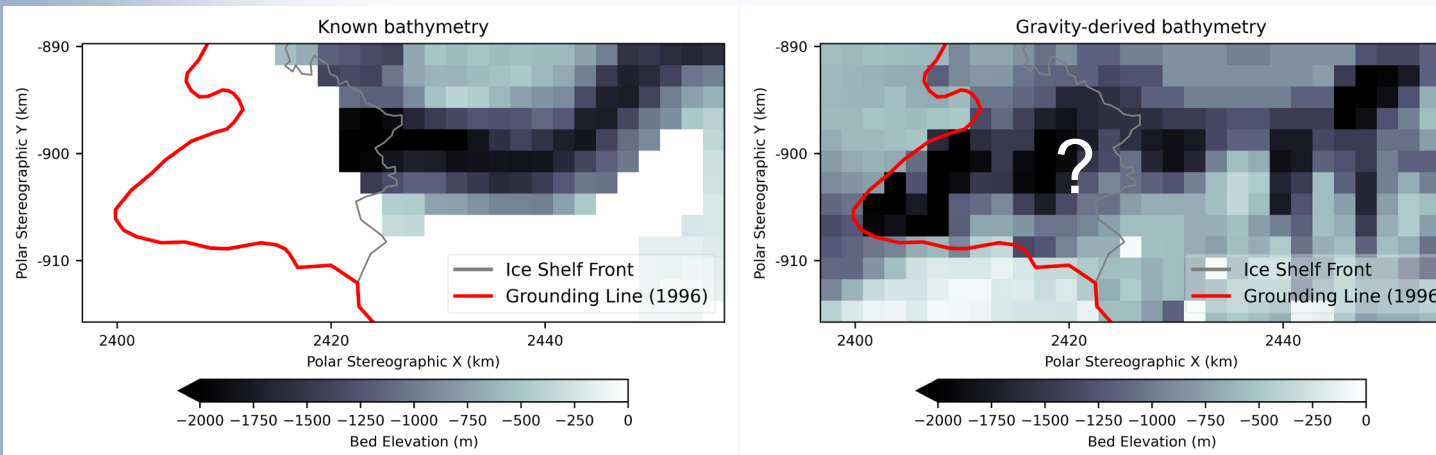


UNIVERSITY OF
WESTERN
AUSTRALIA

Ongoing applications: Gravity-derived Antarctic bathymetry: Vanderford Glacier, East Antarctica

Objective:

- Derive sub-ice-shelf bathymetry using existing aerogeophysical datasets
- Develop open-source workflow that can be applied in other areas of Antarctica

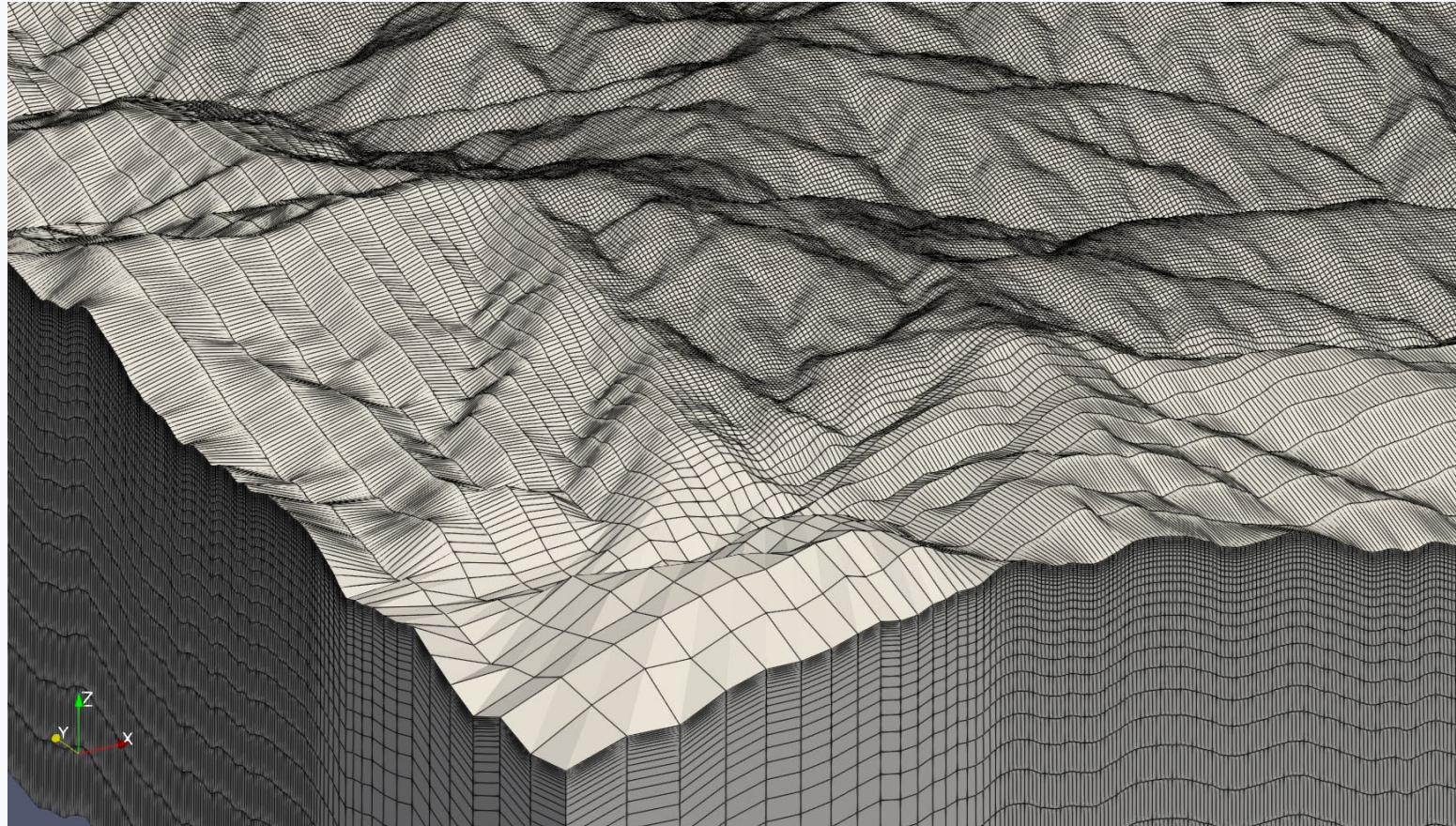
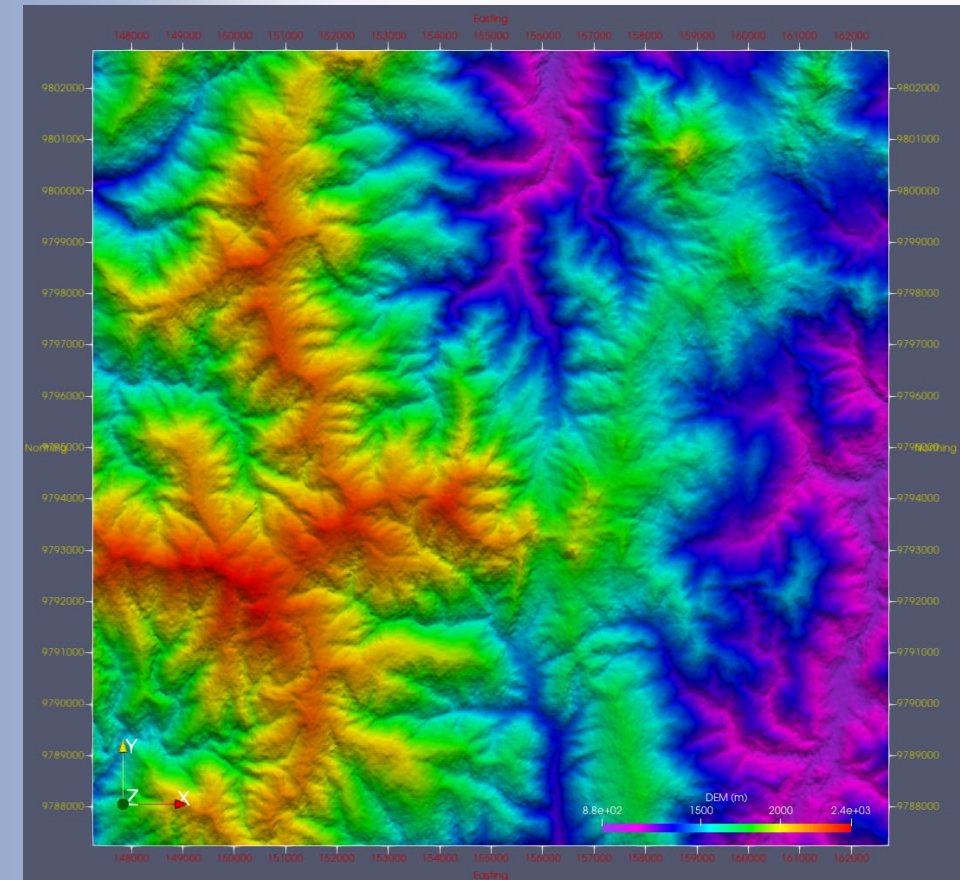


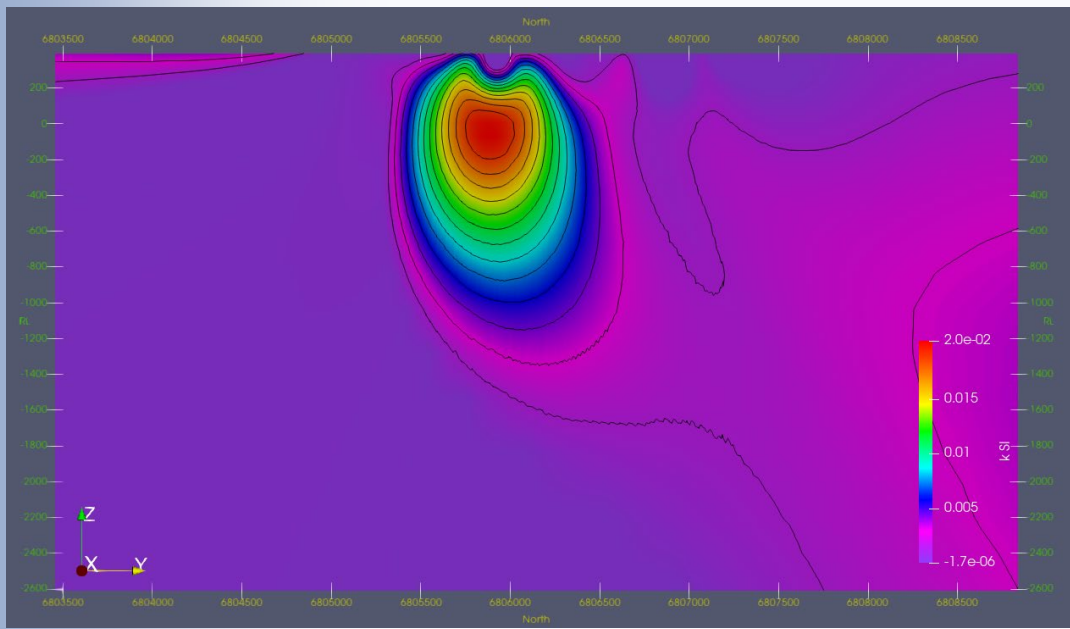
(Courtesy of Lawrence Bird, Monash University)

New features added in Tomofast-x 2.0

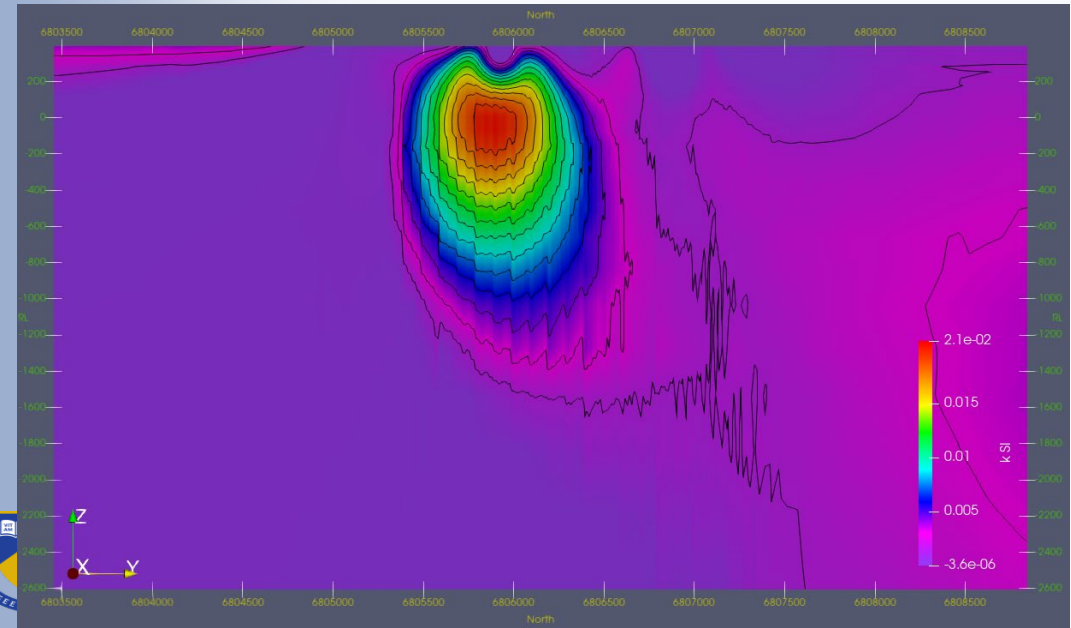
- Topography
- Non-uniform grid
- Wavelet compression
- Magnetisation (remanence) inversion
- Multiple components of magnetic data
- Efficient Parallelisation scheme

Topography & Nonuniform grid



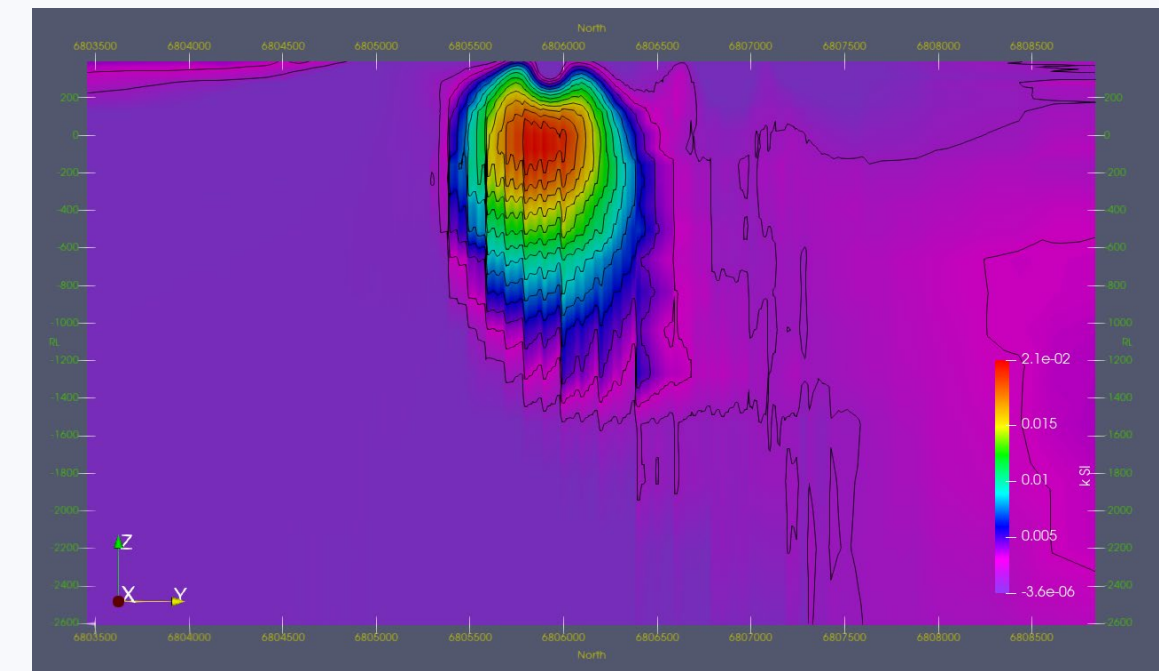


Compression = 1%



Compression = 1%

Wavelet compression



Compression = 0.5%

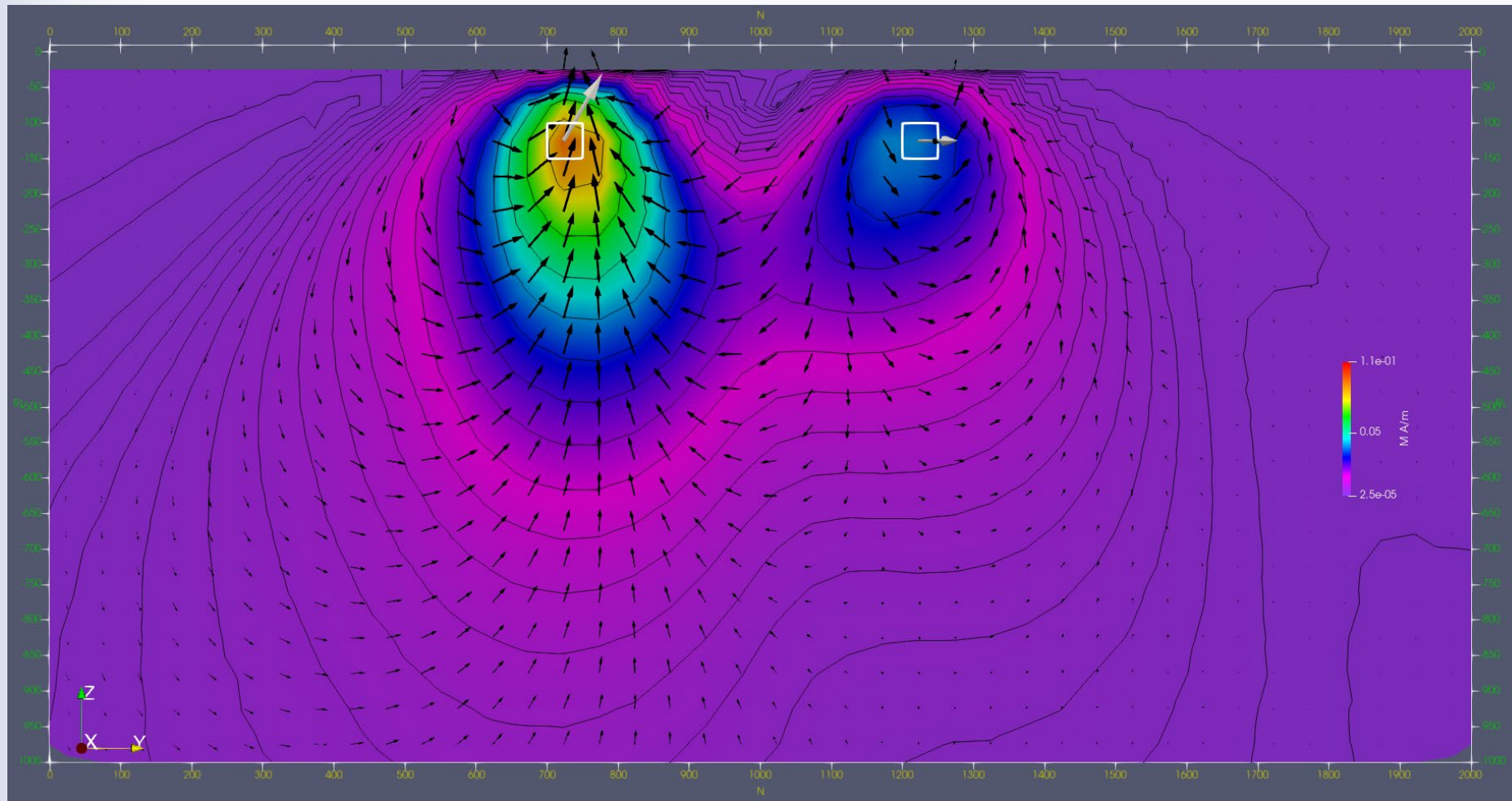
Model size = 242 x 218 x 27
Number of data = 35,200



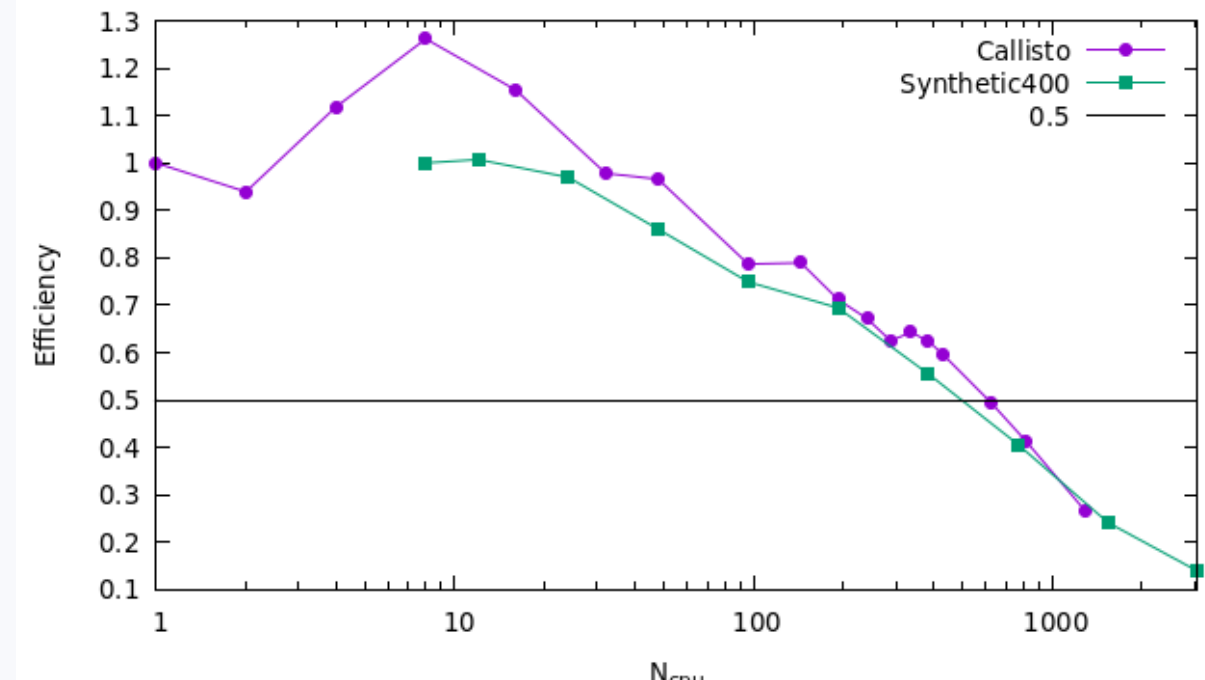
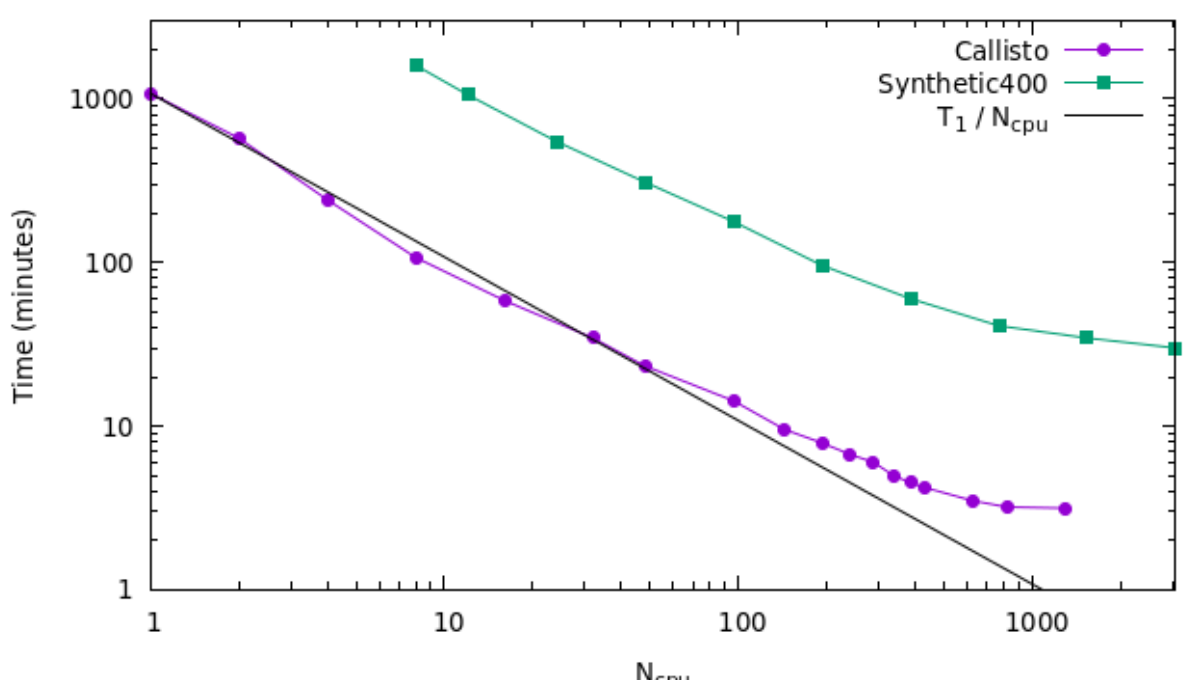
Magnetisation

- Nearly all rocks have a component of **remanent** magnetisation.
- In many cases, the remanent field is strong enough to alter the shape of the observed field.
- A solution: to **invert on magnetisation** rather than susceptibility (Ellis et al 2012).

Magnetisation inversion



Parallel performance



- Callisto model: $242 \times 218 \times 27$, $N_{data} = 35,200$
- Synthetic400 model: $440 \times 440 \times 28$, $N_{data} = 158,006$

Adding drillhole data

Model Setup

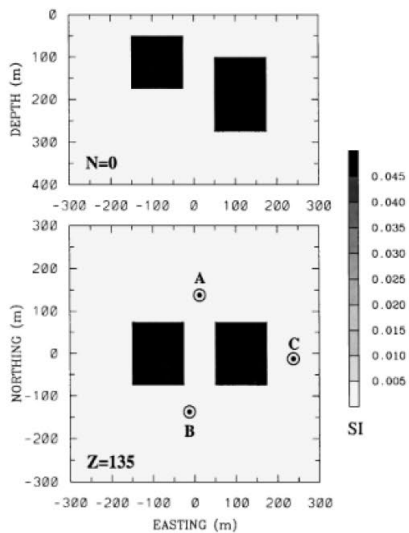
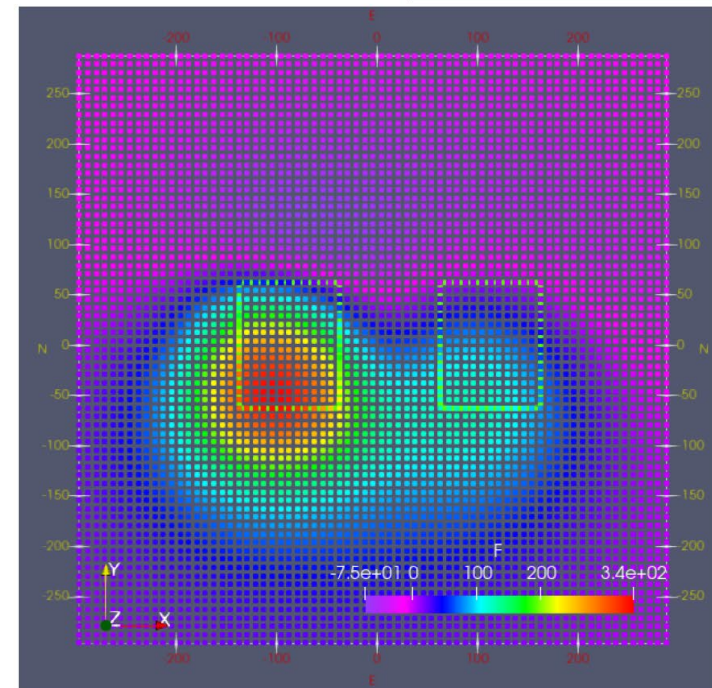
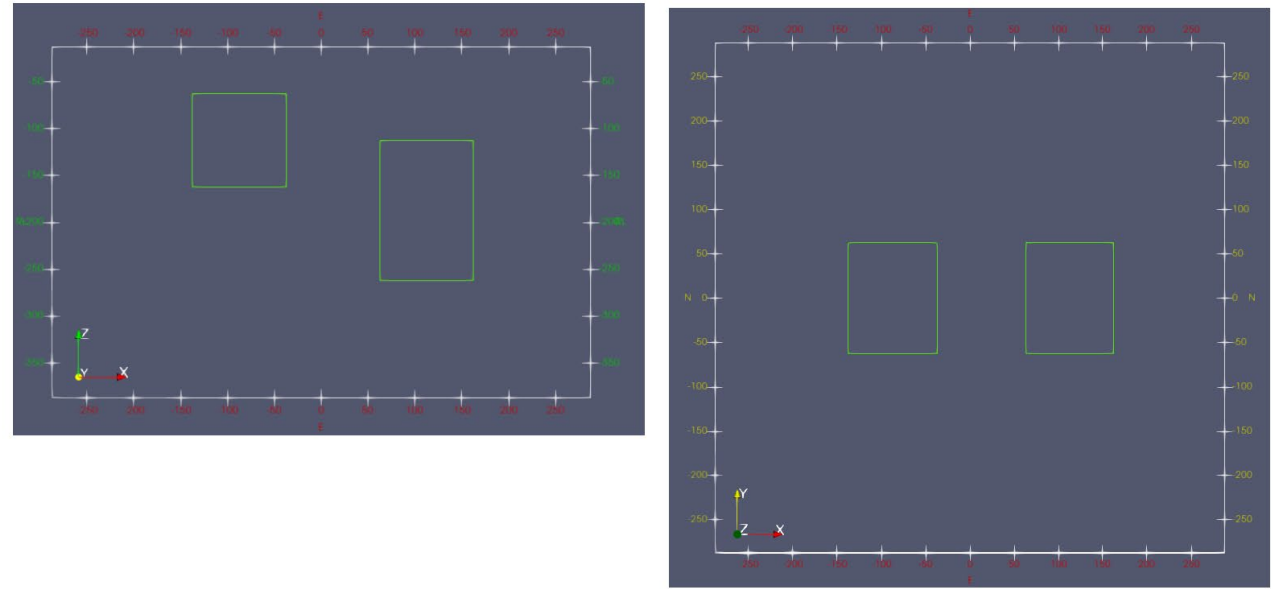
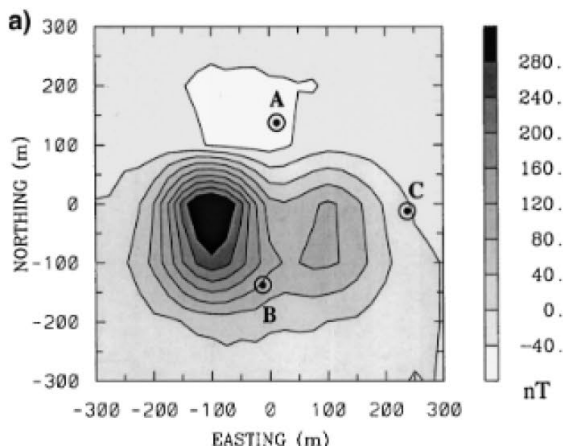


FIG. 1. Two sections of a susceptibility model, consisting of two prisms buried in a uniform background. The collar positions of three vertical boreholes are indicated on the plan section.



Inverting via surface TMI only

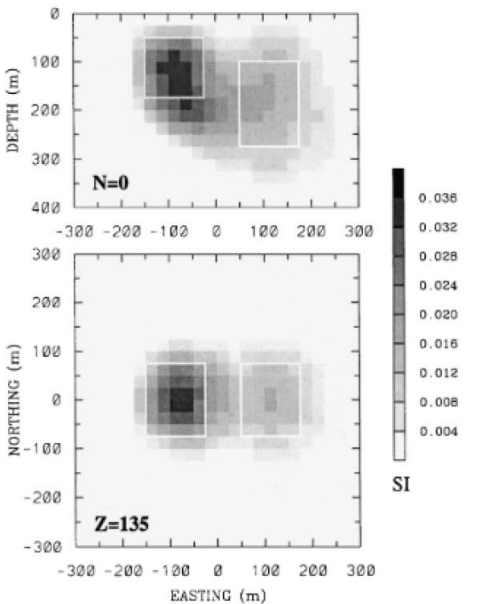
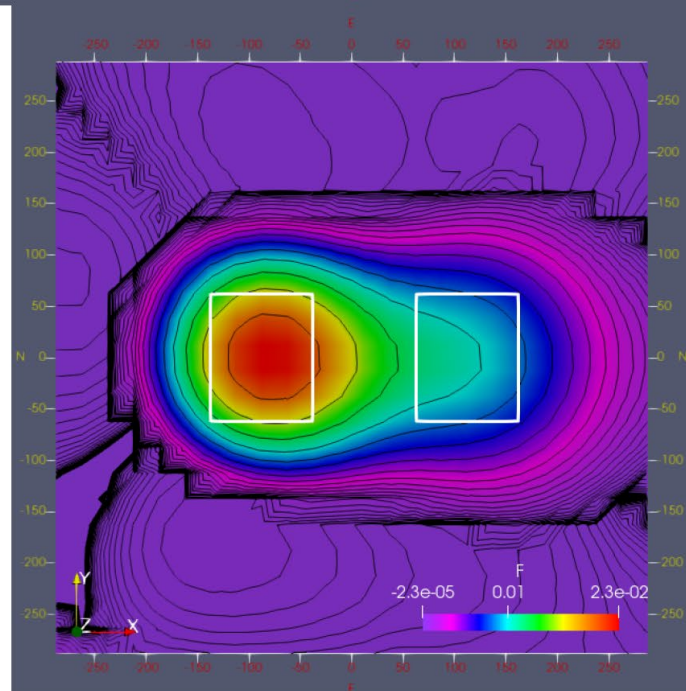
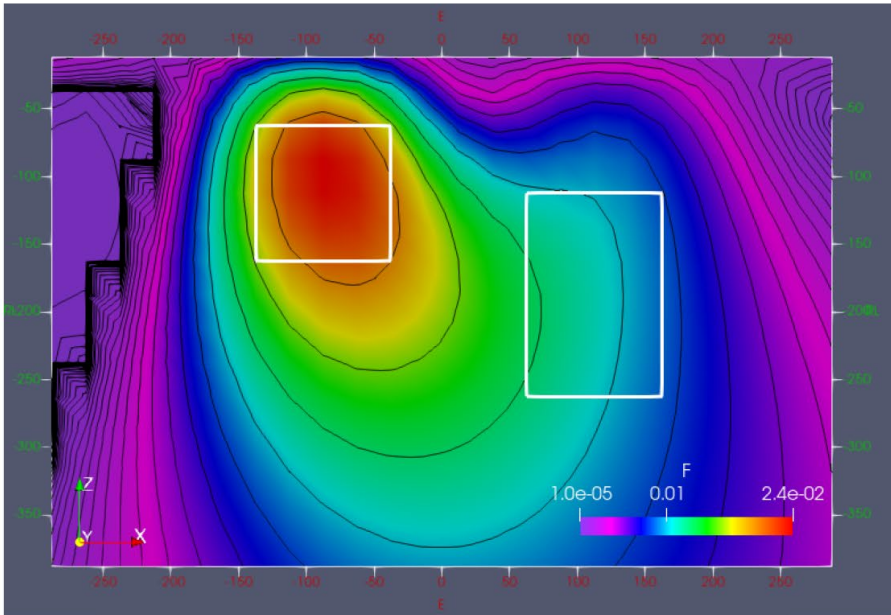


FIG. 5. The susceptibility model recovered from inverting the surface total-field anomaly in Figure 2a using the weighting function shown in Figure 3a. The solid lines indicate the outlines of the prisms. The shallow prism is shown as a high-susceptibility zone with a poorly defined depth extent. The deep prism is shown only as a broad zone of lower susceptibility.



Inverting via 3-component DH data only

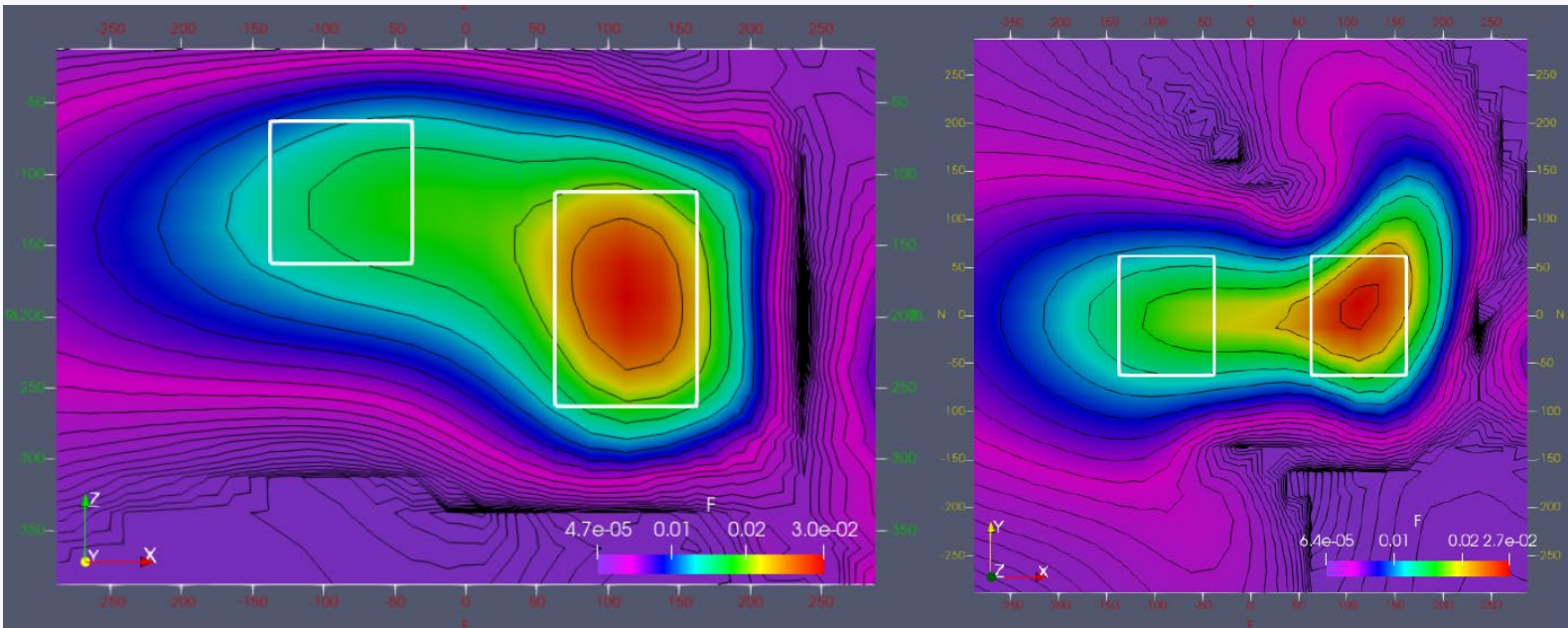
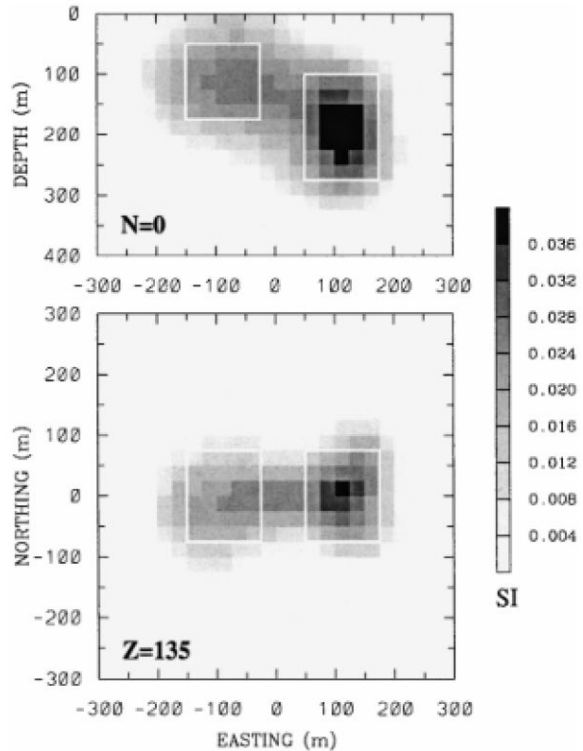


FIG. 6. The susceptibility model recovered from inverting the three-component borehole data in Figure 2b. The definition of the deeper prism is reasonably good since it is close to one of the boreholes.

Inverting via 1-component DH and TMI

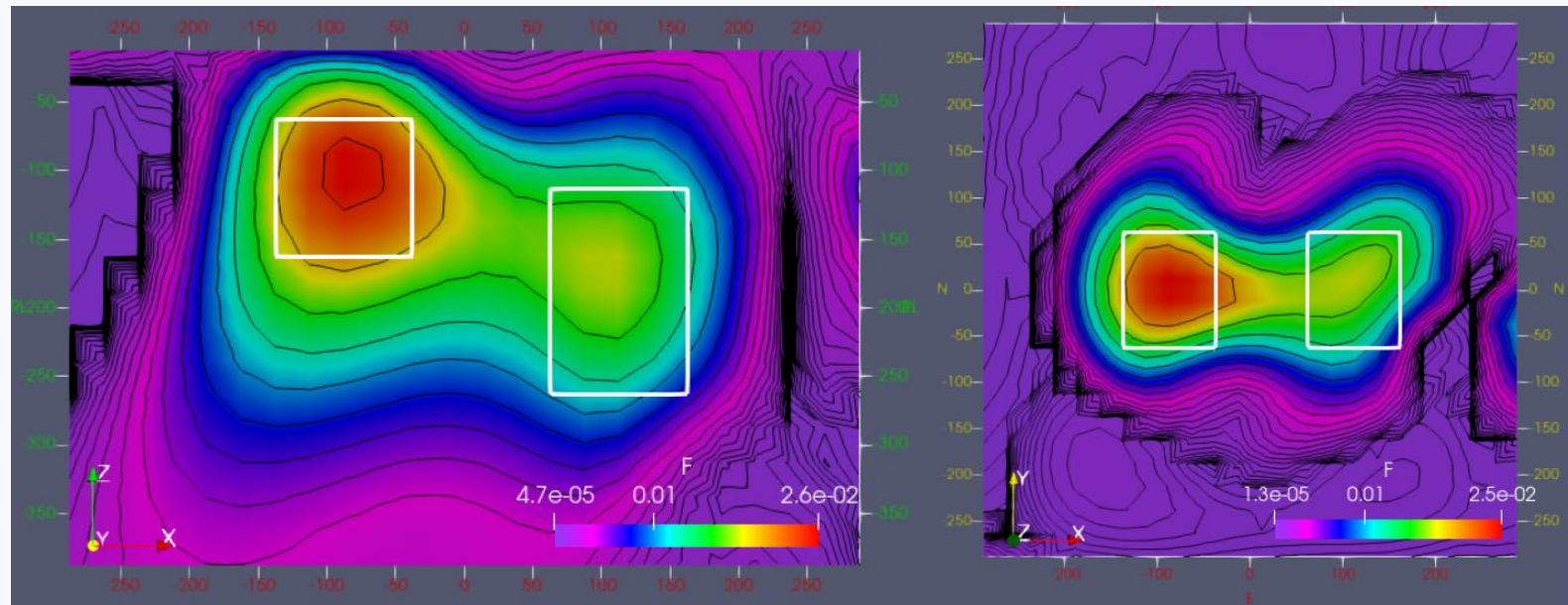
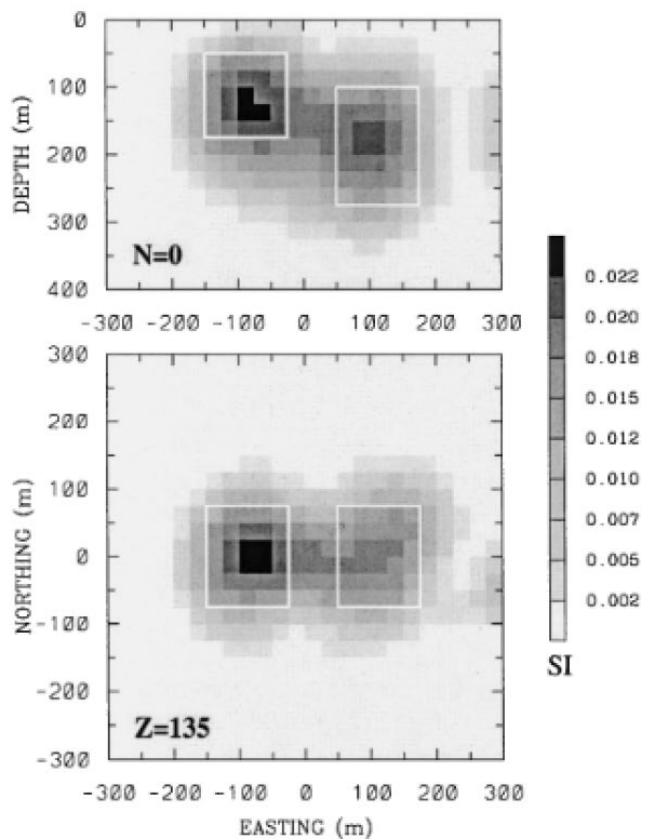


FIG. 9. The susceptibility model recovered from the joint inversion of surface and borehole total-field data. This model is similar to that shown in Figure 7. Both prisms are clearly imaged.

Inverting via 3-component DH and 3-component mag

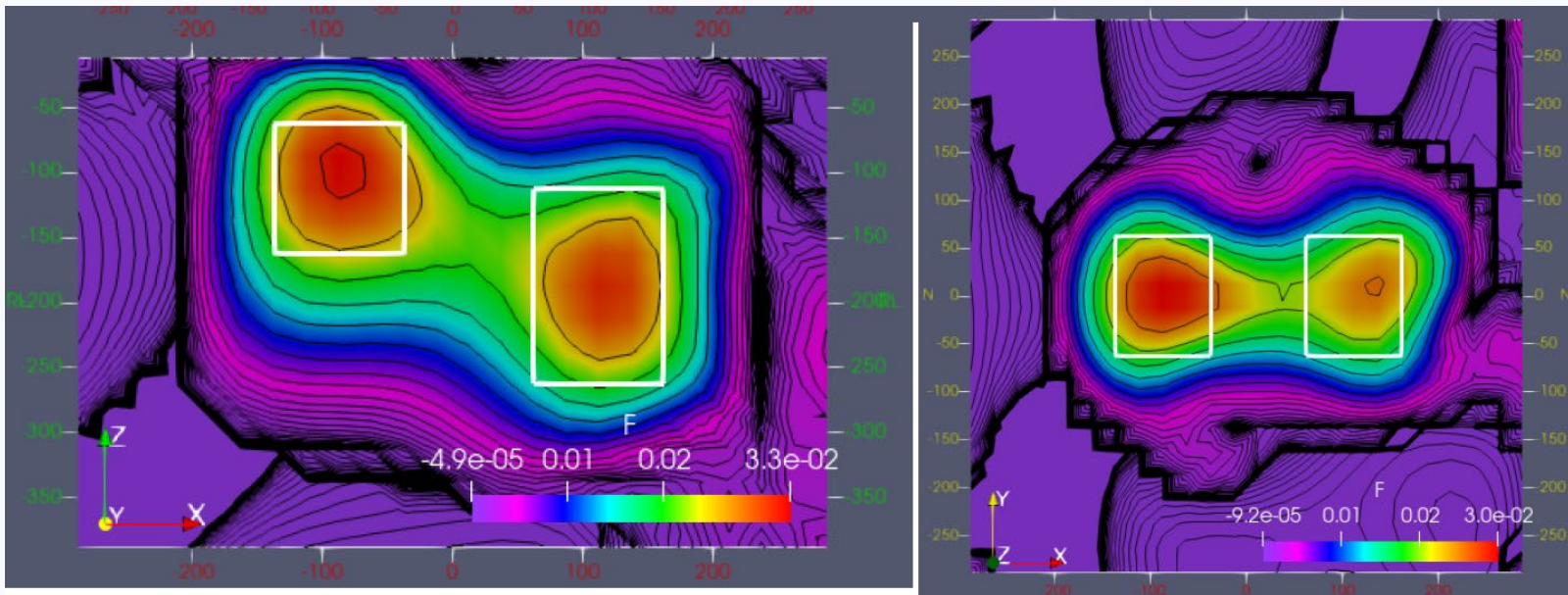
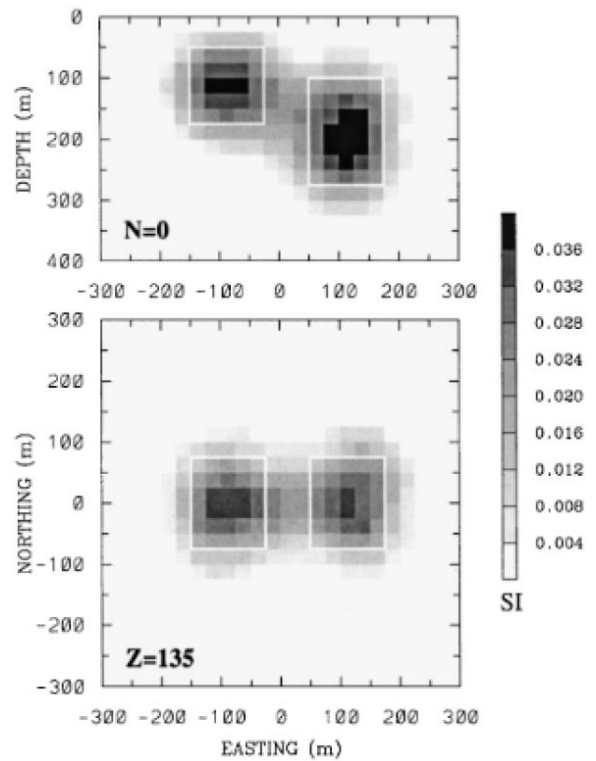


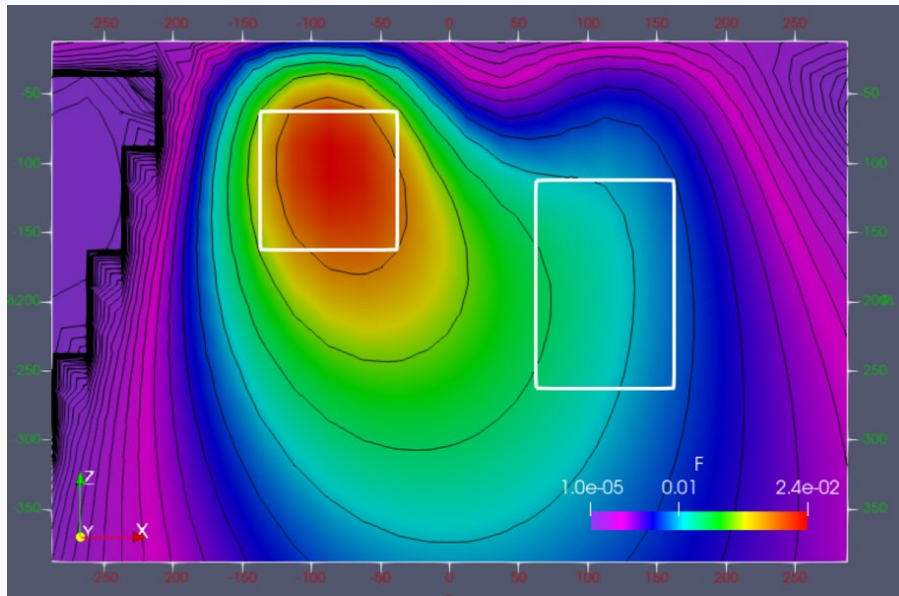
FIG. 7. The susceptibility model recovered from the joint inversion of total-field surface data and three-component borehole data. The sensitivity-based weighting function is used in this inversion. This model clearly defines both prisms and illustrates the improvement achieved by joint inversion of surface and borehole data.



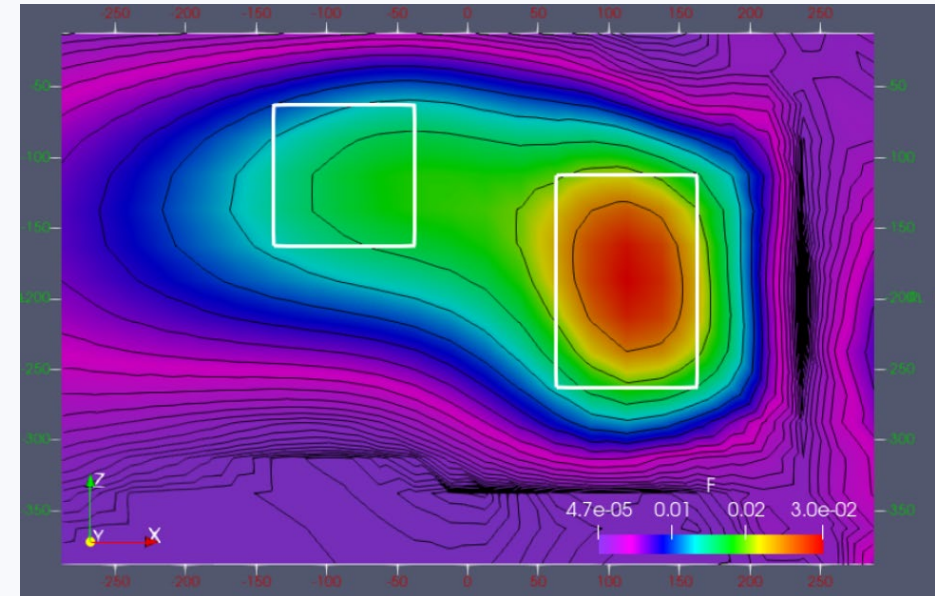
THE UNIVERSITY OF
WESTERN
AUSTRALIA



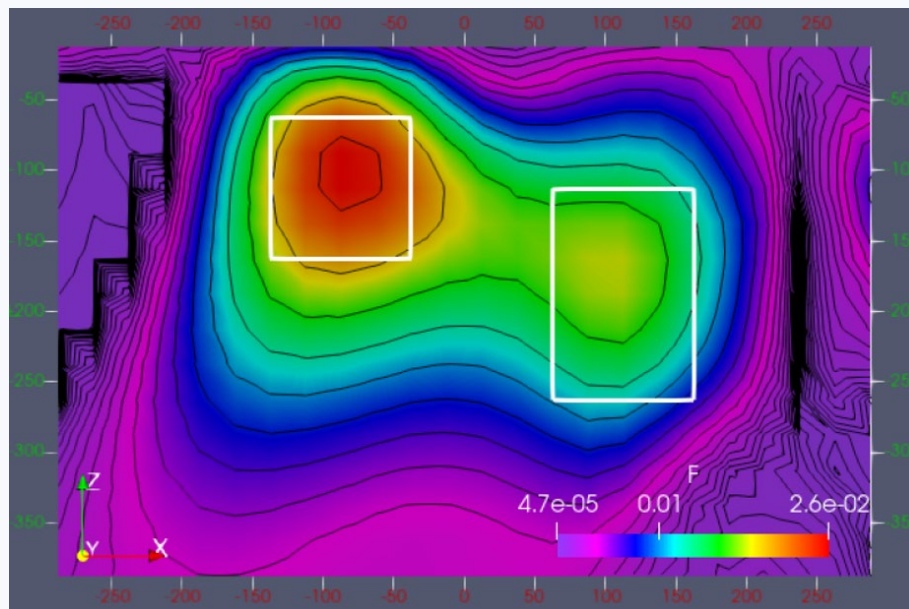
Curtin University



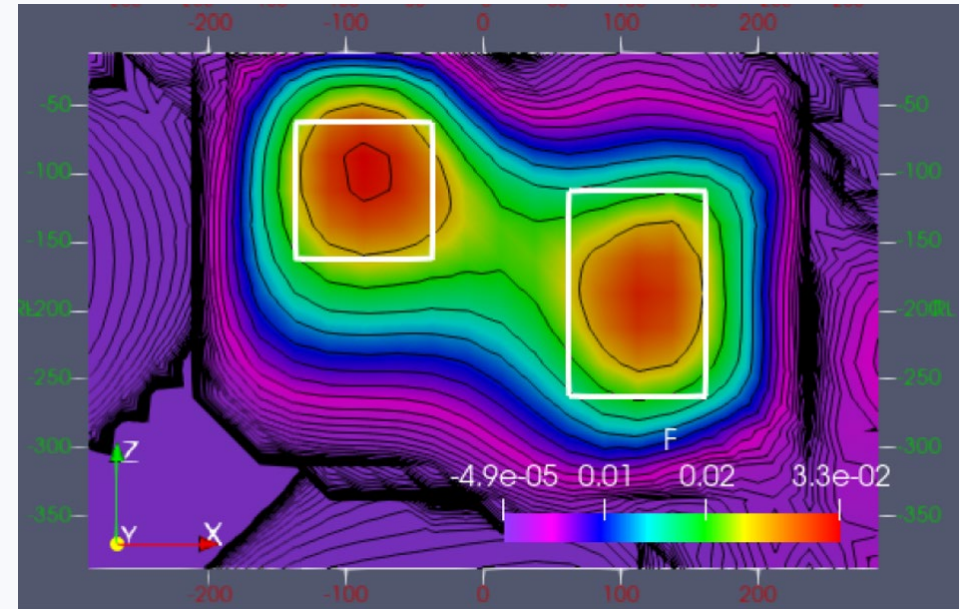
Surface TMI



Drillhole 3-component



Surface + Drillhole TMI



Surface + Drillhole 3-component